THESIS FOR THE DEGREE OF LICENTIATE OF ENGINEERING

Cryogenic Machining of Ti-6Al-4V

SIMON ISAKSON

Department of Industrial and Materials Science

CHALMERS UNIVERSITY OF TECHNOLOGY

Gothenburg, Sweden 2018

Cryogenic machining of Ti-6Al-4V
SIMON ISAKSON

Technical report no IMS-2018-12

Department of Industrial and Materials Science
Chalmers University of Technology
SE-412 96 Gothenburg
Sweden
Telephone + 46 (0)31-772 1000

Printed by Chalmers Reproservice
Gothenburg, Sweden 2018

Cryogenic machining of Ti-6Al-4V

SIMON ISAKSON

Department of Industrial and Materials Science

Chalmers University of Technology

Abstract

The use of cryogenic coolants such as liquid nitrogen or liquid carbon dioxide has emerged as a sustainable alternative to conventional cutting fluids during machining operations, with the potential to increase tool life, leading to productivity gains, as well as to improve the surface integrity of the machined components. In addition, the machined surfaces are left residue-free after the process and there are no used cutting fluids to dispose of. This work aims to increase the understanding of the effects of cryogenic cooling when machining titanium alloy Ti-6Al-4V.

Turning experiments on Ti-6Al-4V revealed that using the same setup (same tool holder and nozzle configuration, comparable coolant pressure) gives very similar results in terms of surface integrity when using cryogenic cooling with liquid nitrogen compared to flood-cooling with emulsion. The choice of coolant did not have a significant impact on surface roughness, microstructure in the near-surface layer or residual stresses. The residual stresses were compressive in all cases, but increased tool wear shifted the residual stress depth profiles towards more compressive stresses. Due to the relatively small nozzle size used, however, the flow of cryogenic coolant was insufficient to match the tool life obtained with emulsion cooling.

In face milling of Ti-6Al-4V with liquid carbon dioxide and emulsion, it was shown that notch wear and chipping were the main wear mechanisms determining the tool life, rather than abrasive wear, i.e. flank wear. Comb cracks were formed in both cooling conditions. However, cryogenic cooling with liquid carbon dioxide greatly delayed the lateral propagation of the comb cracks, thereby delaying the chipping of the cutting edge. Tool life was shown to improve with higher flow rates of coolant, the effect being stronger when using liquid carbon dioxide compared to flood-cooling with emulsion. Moreover, the difference in terms of tool life between cryogenic cooling and flood-cooling with emulsion decreased at higher cutting data.

Keywords: Cryogenic machining, Titanium, Surface integrity, Residual stress, Wear

Preface

This licentiate thesis is based on the work performed at the Department of Industrial and Materials Science between June 2015 and February 2018. The work was carried out under supervision of Adjunct Professor Ibrahim Sadik with co-supervision from Professor Peter Krajnik and Professor Lars Nyborg.

The thesis consists of an introductory part and the following appended papers:

Paper 1: **Effect of cryogenic cooling and tool wear on surface integrity of turned Ti-6Al-4V**
S. Isakson, M.I. Sadik, A. Malakizadi, P. Krajnik
Revised manuscript submitted to 4th CIRP Conference on Surface Integrity (CSI 2018), Tianjin, China, 2018.

Paper 2: **Influence of coolant flow rate on tool life and wear development in cryogenic and wet milling of Ti-6Al-4V**
M.I. Sadik, S. Isakson, A. Malakizadi, L. Nyborg
7th CIRP Conference on High Performance Cutting (HPC 2016), Chemnitz, Germany, 2016.

Paper 3: **The role of PVD coating and coolant nature in wear development and tool performance in cryogenic and wet milling of Ti-6Al-4V**
M.I. Sadik, S. Isakson
Wear. 2017; Vol. 386-387: pp. 204-210.

Contribution to the appended papers:

Paper 1: The candidate participated in the planning of experiments with the co-authors, performed the cutting experiments with the co-authors, performed all characterization work and data analysis, and wrote the paper in cooperation with the co-authors.

Paper 2: The candidate participated in the analysis and interpretation of data, wrote the first draft of the paper and participated in finalizing the paper with the co-authors.

Paper 3: The candidate performed the regression on tool life data, participated in the analysis and interpretation of data, wrote the introduction and participated in finalizing the paper with the co-author.

Contents

1 Introduction

1.1 Background

Since the Brundtland Report introduced the concept of Sustainable Development [1], there has been a growing awareness of the necessity to adopt an all-inclusive view and that economic activities cannot be dissociated from their environmental and social impacts. More recently, "Ensuring sustainable production patterns" is part of the newly adopted Sustainable Development Goals by the United Nations (Goal 12) [2].

Manufacturing is a core component of industrial economies and metal cutting processes are used in all industries to manufacture components of practically any size and shape. Either directly or indirectly, a very large part of all manufactured products involves some machining step. By some estimates, machining processes represent up to 5 % of the GDP in the developed world [3]. On a global level, improving the sustainability of the metalworking industry could have a very significant impact both on the environment and on the health of a large number of workers.

A key sustainability concern in the metalworking industry is the management of cutting fluids (lubricants and coolants), which are often petroleum based. Improper disposal of cutting fluids after use can be very harmful to the environment; proper disposal represents a costly challenge. In addition, the use of cutting fluids can create health risks for workers on the shop floor. Skin irritation and respiratory problems in particular are not uncommon, caused by oil mists and fumes [4]. The use of cryogenic coolants such as liquid carbon dioxide (CO_2) or liquid nitrogen (LN_2) has the potential to eliminate many of these issues. Since they instantly evaporate and dissipate into the atmosphere, the working environment is clean, and there is no used cutting fluid to manage or dispose of. In recent years, research interest in cryogenic machining has grown and promising results have been reported both in terms of tool life and surface integrity of the manufactured component [5].

The aerospace industry is an important driver of technological development in manufacturing. Demand for lighter aircrafts and more fuel-efficient engines necessitates the use of advanced engineering alloys. Titanium alloys, including Ti-6Al-4V, are used both in airframe and engine components, owing to excellent properties such as high strength-to-weight ratio, high toughness, and retained strength at elevated temperatures. These desired properties, combined with low thermal conductivity resulting in high temperatures in the cutting zone, create challenges when machining titanium alloys. For example, the tool wear mechanisms in

machining of titanium are often thermally activated [6]. Titanium alloys have therefore been among the most widely studied in cryogenic machining research.

1.2 Research objectives

The research presented in this thesis aims to increase the understanding of the effects of cryogenic cooling on the results of machining processes in two aspects: (1) there is a lack of publications focused on the residual stresses induced in Ti-6Al-4V after cryogenic machining and (2) whereas most research on cryogenic machining has been conducted on turning operations, fewer results have been published for milling.

In particular, the specific objectives are:

- For turning, to examine the influence of cryogenic cooling with liquid nitrogen on the surface integrity of Ti-6Al-4V including residual stresses.
- For milling, to investigate the wear development, wear mechanisms and tool life resulting from cryogenic cooling with liquid carbon dioxide. Which cutting conditions, including flow rate of the coolant, coating of the tool and cutting data offer the highest potential for improving the process compared to flood cooling with an emulsion?

2 Fundamental aspects of machining

2.1 Turning and Milling

Machining refers to operations in which thin chips are removed by one or several tool edges from a body of material, the workpiece [7]. Two of the principal machining processes are turning and milling, which differ by the primary method used to create relative motion between the workpiece material and the cutting edge. In turning, the workpiece rotates and the tool is brought in contact with the workpiece. In contrast, in milling, the tool rotates to bring the cutting edges into contact with the workpiece. Additionally, a key difference between turning and milling is that turning uses a single point tool, whereas multiple cutting edges are used in milling. Consequently, the turning tool is in general continuously engaged during operation. Milling, however, is an interrupted cutting operation, since the cutting edges enter and exit the workpiece as the cutter rotates. The two machining operations used in this work are longitudinal turning and face milling. In longitudinal turning, the direction of feed of the tool is parallel to the axis of rotation of the workpiece. During face milling operations, the direction of feed of the workpiece is perpendicular to the axis of rotation of the cutter. These processes are illustrated in figure 1.

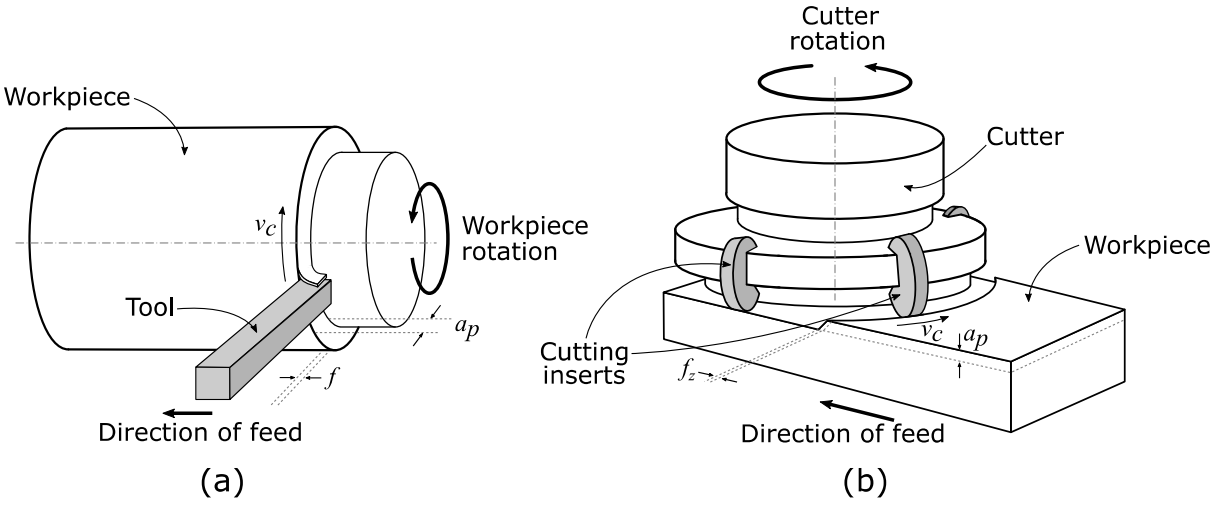

Figure 1: Illustration of the two machining operations used in this work: (a) longitudinal turning and (b) face milling. Some important process parameters are: cutting speed (v_c), feed (f), feed per tooth (f_z) and depth of cut (a_p).

Figure 2a shows a schematic representation of the cutting zone, where the workpiece, tool and chip are in contact. The chip formation process occurs due to the relative motion of the workpiece material (v_c) onto the tool. Plastic deformation and severe shearing take place, particularly in the shear plane (shear zone 1) where the workpiece to chip transition occurs. Strong deformations also occur at the tool-chip interface on the rake face of the tool (shear zone 2) and along the new cut surface (shear zone 3) [8].

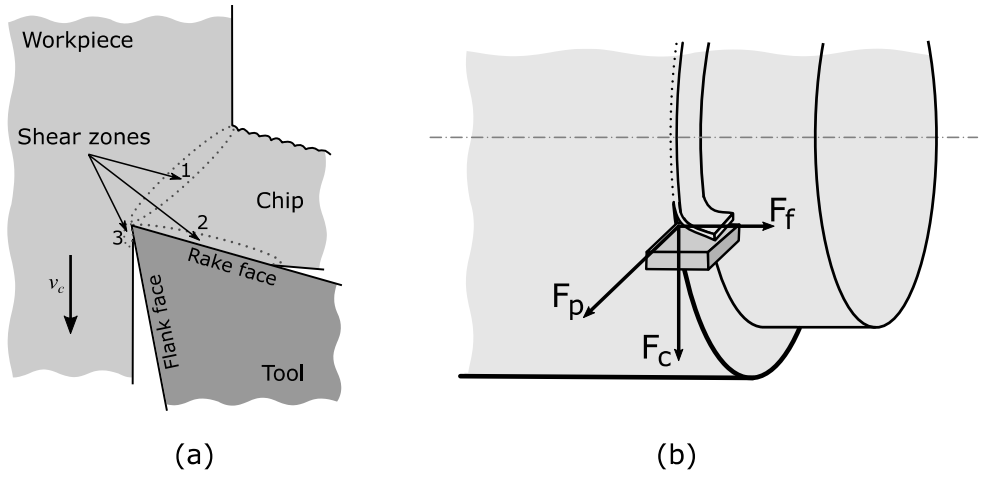

Figure 2: Illustration of (a) the cutting zone with chip formation and shear zones and (b) the three perpendicular components of the force acting on the cutting tool: F_c cutting force, F_f feed force and F_p passive force. Adapted from [8].

The mechanical work involved in the chip formation process is almost entirely converted into heat [7]. Much of the heat is carried away by the chips. Still, the resulting high temperatures in the cutting zone and on the tool have a direct influence on the tool life (rate of wear), on the friction at the tool-chip interface, as well as on the performance and quality of the machined part [9].

The resultant force acting on the cutting tool during the machining process can be separated into three components as illustrated in figure 2b for longitudinal turning. The cutting force F_c acts in the direction of rotation of the workpiece, the feed force F_f acts in the direction opposite to the feed f and the passive force F_p acts in the radial direction, pushing the tool away from the workpiece.

2.2 Cooling technology and cutting fluids

The heat generated in metal cutting is of primary concern and has a strong influence on the machinability of the workpiece material in terms of tool wear and quality of the machined surface. In many applications, the use of cutting fluids during machining operations is a requirement in order to achieve acceptable tool life and surface quality. These fluids act as coolants and/or lubricants. According to Trent [7], there are four objectives to the use of cutting fluids:

1. To prevent the tool, workpiece and machine from overheating and distorting,
2. To increase tool life,
3. To improve surface finish,
4. To help clear the chips from the cutting area.

The relative importance of the lubrication and cooling effects of the cutting fluids generally vary with the cutting speed. At lower cutting speeds, the main function of the cutting fluid is lubrication. The heat generation being more intensive at higher cutting speeds, the cooling effect of the cutting fluid becomes most important [9]. Another consideration is that at high cutting speeds, the cutting fluid simply cannot penetrate the cutting zone effectively to provide lubrication.

Cutting fluids have traditionally been classified into two main categories: oil-based and water-based or water-miscible fluids [9]. The water-based cutting fluids can further be divided into emulsifiable and water-soluble fluids. Whereas oil-based cutting fluids usually are supplied ready to use, the water-based fluids are normally delivered in concentrate form. Once mixed with water, they form an emulsion or a solution. Gaseous coolants can be considered a third main category of cutting fluids. The classification of cutting fluids is illustrated in figure 3a.

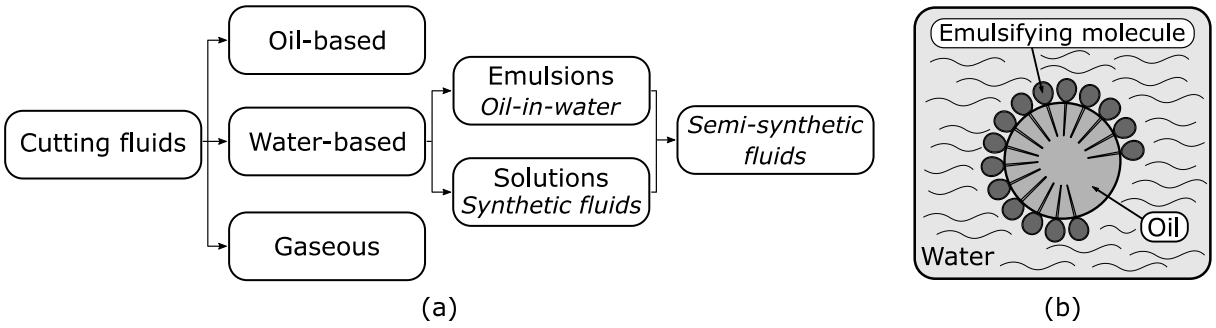

Figure 3:(a) Classification of cutting fluids. Adapted from [9]. *(b) Illustration of an oil-in-water emulsion. Adapted from* [10].

2.2.1 Straight oils

Oil-based cutting fluids, also called straight or neat oils, are primarily mineral oils but can be blended with animal fats and vegetable oils. They may also include a number of additives to improve the performance, such as sulfur, chlorine and phosphorous. Mineral oils are excellent lubricants, especially when blended with fatty oils [9]. Oil-based cutting fluids also offer protection against corrosion. They are however comparatively poor at dissipating heat, can be a fire hazard, and create oil mist, which is detrimental to the working environment [11].

2.2.2 Emulsions

A cutting fluid is an emulsion if it is composed of a suspension of oil droplets in water. The oil is blended with emulsifying agents (emulsifiers) that are necessary to form the oil droplets and keep them suspended in water. The emulsifiers are bipolar molecules, with a hydrophilic head and a hydrophobic tail, lining up to form a film around the oil droplets (see figure 3b). This

prevents the droplets from merging and separating from the water to form a surface layer in the tank [10].

The stable oil-in-water emulsion formed then combines the lubricant properties of oils with the cooling capabilities of water. The advantage of emulsifiable oils over straight oils is thus a greater heat dissipation, combined with improved working conditions (cleaner workshop environment, reduced misting and fire hazard) [11,12]. Commonly used additives are corrosion inhibitors, anti-foaming agents, and bactericides/microbiocides.

2.2.3 Synthetic cutting fluids

Synthetic cutting fluids are chemical solutions, diluted in water, that contain no mineral oils. The chemicals in solution can be corrosion inhibitors (amines and nitrites), water softening (phosphates and borates), lubricants, wetting agents, and germicides [12]. Synthetic cooling fluids provide excellent cooling but in counterpart suffer from a lack in lubrication capability [11].

2.2.4 Semi-synthetic cutting fluids

Semi-synthetic cutting fluids are essentially a combination of synthetic cutting fluid with emulsion or soluble oil. As such, they combine the characteristics of both types of cutting fluids.

2.2.5 Gaseous coolant lubricants

Gas-based coolants such as air, nitrogen or carbon dioxide have been used as an environmentally friendly alternative. Inert gases may prevent oxidation of the tool at high cutting temperatures [11]. Due to low thermal conductivity however, the cooling capability of gases is low compared to liquids [13]. The use of cooled air or other gases attempts to improve the cooling capability while taking advantage of the fact that gases may be better able to penetrate the cutting zone than liquid cutting fluids [11].

2.2.6 Issues with the use of cutting fluids.

There are both health and environmental issues related to the use of cutting fluids in machining operations. Skin exposure as well as inhalation of cutting fluid mist can represent serious health hazards for machine operators [4]. Depending on the application, only a portion of the cutting fluid applied to the cutting zone may affect the cutting process. In some cases, a large part of the cutting fluid used will form an aerosol in the environment of the machine, contributing to pollution and exposing operators to mist. The mechanism of mist formation can be modeled in two forms: atomization and vaporization/condensation, as illustrated in figure 4 [14]. Atomization can take place through interaction with machine parts, either stationary or rotating.

Exposition to high temperature surfaces leads to the vaporization of some amount of cutting fluid, with subsequent condensation into mist droplets. The production and disposal of the cutting fluids also represent environmental challenges.

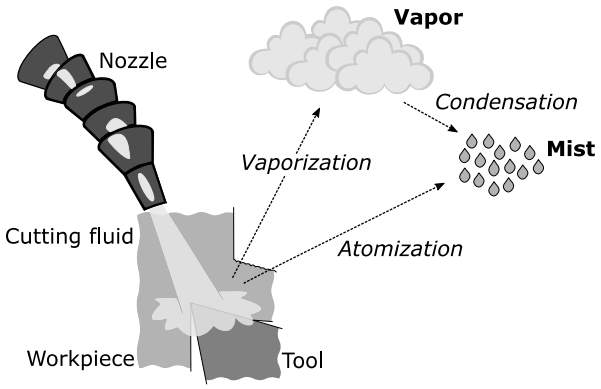

Figure 4: Mechanisms of cutting fluid mist formation. Adapted from [14].

2.2.7 Application of cutting fluids

Flood cooling

The most common method of supplying cutting fluids is by flooding the tool, workpiece and cutting zone. The cutting fluid is supplied in a steady stream through nozzles directed at the tool-work or tool-chip interfaces. The nozzles can be external or integrated to the tool, tool holder or spindle, and the cutting fluid is recirculated in the machine.

High pressure coolant lubricant supply

In flood cooling, the cutting fluid is supplied somewhat uncontrolled and mostly reaches the top-side of the chip. The coolant may not penetrate the cutting zone nearest the cutting edge, where the heat generation is greatest. An effective alternative is high pressure fluid supply, where a jet of cutting fluid is supplied at high pressure directed toward the tool-chip interface on the rake face and/or the tool-work interface on the flank face [15]. Many researchers have reported positive results, especially for machining demanding materials used in the aerospace industry such as nickel superalloys [16] and titanium alloys [17]. For instance, Ezugwu et al. reported 111-123 % improvement in tool life with coolant supply pressures of p=20.3 MPa and p=11 MPa compared to flood cooling when finish turning Ti-6Al-4V with uncoated carbide tools [18].

Minimum Quantity Lubrication

Worker health and environmental issues, as well as the costs associated with the use of cutting fluids in the machining process, are driving factors behind the desire to reduce the consumption

of cutting fluids. The development of Minimum Quantity Lubrication (MQL) for high performance machining is an important area of research [19]. In this process, small amounts of cutting fluid is directed to the tool and cutting zone via a nozzle in aerosol form. MQL was mostly implemented for automotive materials like gray cast iron, but lack of sufficient cooling is a challenge when machining high temperature alloys [15,19]. Promising results have been reported for machining of Ti-6Al-4V using MQL with additives [20,21] or combined with additional cooling (cold air) [22].

2.3 Tool wear

During the cutting process, the tool material is subjected to high mechanical and thermal loads. Tool wear is the progressive damage (i.e loss of cutting tool material, change in geometry) on the tool that occurs as a result of those thermo-mechanical loads [9]. It is an essential parameter to evaluate the performance of the cutting tool, as tool wear not only influences the machining costs, but also the quality and performance of the machined parts. This section provides a brief overview of different types of tool wear and the underlying wear mechanisms.

2.3.1 Forms of tool wear

The gradual damage of the tool material occurs mainly on the tool's flank and rake faces. Some common forms of tool wear are illustrated in figure 5:

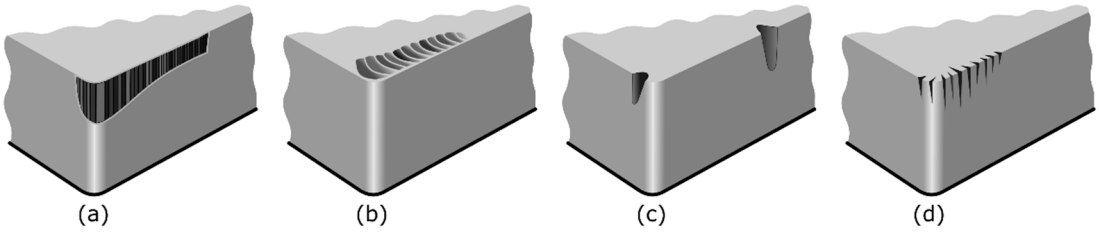

Figure 5: Illustration of different types of tool wear: (a) flank wear VB, (b) crater wear KT, (c) notch wear VB_N, (d) thermal cracking (comb cracks). Adapted from [23].

Flank wear

Wear appears on the clearance face of the tool as a result of the continuous sliding against the new generated surface of the machined component. It takes the form of a loss of relief angle i.e. the contact area between the tool and new surface increases. This leads to increased friction resistance [13,23].

Crater wear

Crater wear occurs on the rake face, in the contact zone between the tool and the chip. The crater depth is normally greatest at the midpoint of the contact zone, where the highest temperature on the tool is found [13,23].

Notch wear

Notch wear is typically located at the depth-of-cut on the major and minor cutting edges. It often occurs when machining materials prone to work hardening and is aggravated by high temperatures and the presence of oxygen [23].

Thermal cracks

In interrupted cutting operations such as milling, the cutting edge of the tool is exposed to repeated heating and cooling cycles, as it enters and exits the work material. Large fluctuations in temperature, as well as high temperature gradients are thus created. Thermal cracks develop as a result of thermo-mechanical fatigue [9,23]. These cracks form along the rake and flank face, perpendicular to the cutting edge, and are sometimes called 'comb cracks'. Subsequent cracks may appear parallel to the cutting edge, joining with the comb cracks and leading to chipping and/or spalling, severely reducing the tool life [9,23,24].

2.3.2 Tool wear mechanisms

The appearance and progression of tool wear can be attributed to a number of different mechanisms, including abrasion, adhesion, thermal or mechanical stress and fatigue, and diffusion [8]. The different processes often overlap in their effect on tool wear.

Abrasion

Abrasive wear involves loss of material and is due to the sliding of hard particles against the tool. The hard particles can in principle have three origins: from the microstructure of the workpiece material (i.e. carbides and inclusions), broken-off material from the tool itself, or formed by a chemical reaction between the chips and cutting fluid [9].

Adhesion

Adhesion wear occurs as a result of the tool material and the work material forming bonds: micro-welds are formed in the cutting zone. The relative motion between the tool and workpiece leads to the deformation and shearing off of these bonds. If the material separation occurs on the tool, the loss of tool material is referred to as adhesion wear [8].

Stress and fatigue

Mechanical and thermal stresses lead to damages on the cutting edge in the form of chipping, notching, cracks or plastic deformation. The damage can occur directly if the stress is above the strength or deformation resistance of the tool material, or over a period of cyclical stress (fatigue). [8]

Diffusion

Diffusion is a thermally activated process where individual atoms change position. The high temperatures and pressures in the contact zone between the tool, workpiece and chip can lead to diffusion taking place between the tool and work materials. Direct loss of tool material by diffusion may be small but possible to quantify as wear. More importantly, diffusion in either direction (i.e. work material into the tool or alloying elements of the tool material into the workpiece/chips) leads to a change in the composition of the tool material. Characteristics such as hardness can change, resulting in reduced wear resistance and increased wear rate. [8]

2.4 Machinability

The term *machinability* can intuitively be understood as referring to the ease or difficulty with which a particular workpiece material can be machined. However, there is no specific and intrinsic property of the material that can be used to quantify machinability. Since the physical processes that take place are affected by the whole machining system, the specific cutting conditions and setup also have to be taken into account. Trent proposes that machinability can be assessed by the following criteria [7]:

- Tool life
- Limiting rate of material removal
- Cutting forces
- Surface finish
- Chip shape

As such, what constitute good machinability may vary with context.

2.5 Surface integrity

There is a strong relationship between the machining process, the quality and properties of the machined surface, and the functional performance of the machined part. The term *surface integrity*, which was coined in 1964 by Field and Kahles [25] highlights this link. They later provided a structured set of parameters to evaluate surface integrity, presented in table 1.

Table 1: Surface integrity (SI) data set developed by Field and Kahles [26].

Minimum data set	Standard data set	Extended data set
1. Surface finish	1. Minimum SI data set	1. Standard SI data set
2. Macrostructure (10x or less) a. Macrocracks b. Macroetch indications	2. Fatigue tests (screening) 3. Stress corrosion tests	2. Fatigue tests (extended to obtain design data) 3. Additional mechanical tests a. Tensile b. Stress rupture c. Creep d. Other specific tests (e.g. bearing performance, sliding friction evaluation, sealing properties of surfaces)
3. Microstructure a. Microcracks b. Plastic deformation c. Phase transformations d. Intergranular attack e. Pits, tears, laps, protrusions f. Built-up edge g. Melted and redeposited layers h. Selective etching	4. Residual stress and distortion	
4. Microhardness		

The surface integrity data set shows the large number of parameters related to surface integrity. The minimum data set, covering surface finish, metallographic information and hardness measurements, provides a relatively inexpensive first assessment of the surfaces. More in-depth data is provided by the standard data set, which includes more expensive and time-consuming tests. The extended data set provides data necessary for engineering design applications. A relevant set of parameters should be chosen based on the specific requirements of the component as well as the workpiece material and machining process used.

Surface integrity thus refers to topography (surface roughness), metallurgy (microstructure), mechanical properties (hardness, residual stresses, fatigue) and chemistry (corrosion resistance). In the case of machining of titanium alloys, these parameters have been studied in a number of publications. There are reviews available giving an overview of the topic [27–29].

2.5.1 Residual stresses

Residual stresses are the internal stresses that remain, self-equilibrating, in a free body when no external forces or constraints are applied. The machining process causes strong plastic deformation in the surface layer of the work material, producing plastic strains. The bulk of the work material on the other hand sees only minimal plastic deformation and has a constraining effect. Residual stresses are caused by the elastic response of the material to the inhomogeneous distribution of nonelastic strains. Thermal expansion strains, precipitation, phase transformation or misfit also cause nonelastic strains contributing to residual stresses [30].

Machining induced residual stresses are of great concern to the functional performance of the machined part, as they have an influence both on the static and dynamic strength of the component. Their presence can thus greatly affect the service life of the machined component, potentially leading to its premature failure. Residual stresses act like a pre-stressor, effectively lowering the yield stress of the material (risk of static fracture) [31]. Tensile residual stresses also undermine fatigue strength not only because the mean stress is increased, but also because their presence favors crack nucleation and propagation. Conversely, the presence of compressive residual stresses improves fatigue life.

Residual stresses can also lead to deformations after machining, particularly in thin workpieces. Depending on the material and environment, tensile residual stresses may favor stress corrosion [31].

In advanced applications, where high demands are placed on strength (static and dynamic) and dimensional accuracy, the control of residual stresses is thus essential.

3 Titanium alloys and applications

The development of titanium alloys and the history of their use in commercial applications has been intimately linked to the aerospace industry, starting in the early 1950s with the first significant use in a jet engine (Pratt & Whitney J-57). To this day, the single largest application for titanium remains in the aerospace industry. The main appeal of titanium alloys and the principal reason for their early adoption and large use by the aerospace industry is their high strength-to-weight ratio. In addition, their strength is maintained at elevated temperature. Several other properties of titanium alloys offer performance advantages in a wide array of applications. Great corrosion resistance is useful for industrial and petrochemical applications, as well as for use in marine vessels. In medical and dental applications, titanium is widely used in implants and prosthesis, thanks to its biocompatibility. The combination of low density, high strength and low stiffness makes titanium an attractive material for sporting goods. [32]

3.1 Physical metallurgy and common titanium alloys

Pure titanium is an allotropic element, meaning that more than one crystallographic form is possible. At room temperature, titanium exhibits a hexagonal close packed (hcp) crystal structure, known as the alpha (α) phase. At 888 °C, a transformation occurs and above this temperature, titanium has a body-centered cubic (bcc) crystal structure, referred to as the beta (β) phase [33]. The unit cells of the alpha and beta phases are illustrated in figure 6. The addition of alloying elements can have an effect on the β transus temperature. Alloying elements are thus classified as α-stabilizers when they increase the transition temperature (increase the temperature at which the α phase is stable) and as β-stabilizers when they lower the transition temperature (lower the temperature at which the β phase is stable). Among α-stabilizers are aluminum, carbon, oxygen and nitrogen. Examples of β-stabilizers are vanadium, molybdenum, niobium, iron, chromium, nickel, cobalt, and copper among others.

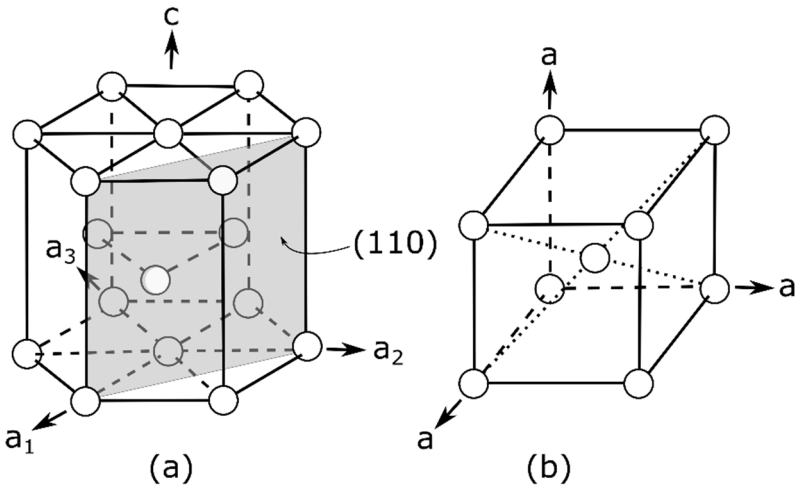

Figure 6: Unit cells of the two phases of titanium: (a) hcp α phase and (b) bcc β phase. The plane used to determine residual stresses by X-ray diffraction is marked in the α phase (see section 5.2.1). Adapted from [34].

Titanium alloys are commonly classified, according to the phases present, into three categories: α, α+β and β alloys [34]. These categories are shown in the pseudobinary phase diagram in figure 7, where the composition is schematically given as the amount of β stabilizing alloying element.

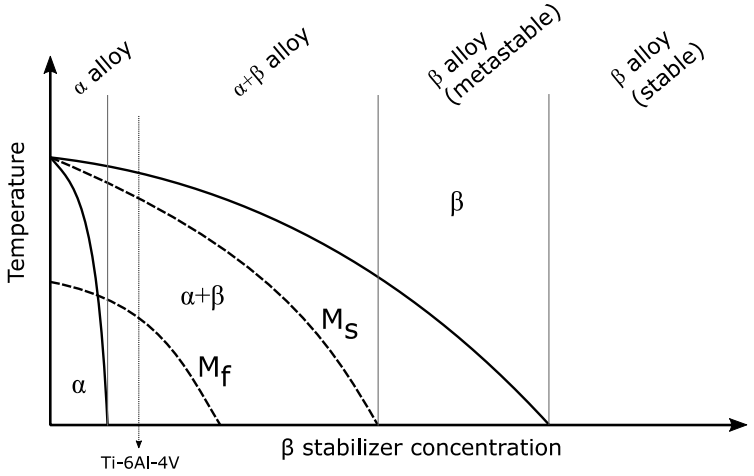

Figure 7: Pseudobinary titanium phase diagram (schematic) showing the different categories of titanium alloys. The approximate position of alloy Ti-6Al-4V is also shown. Adapted from [33].

The workpiece material used in this thesis is the α+β alloy Ti-6Al-4V. It is perhaps the most commonly used titanium alloy, accounting for more than half of the titanium sold in Europe and the United States. Ti-6Al-4V represents 60 % of the titanium used in jet engines and up to 90 % of the titanium used in airframes [35].

The maximum operating temperatures under creep conditions for Ti-6Al-4V are about 300-450 °C. Above and up to 500-600 °C, near α alloys such as Ti-6Al-2Sn-4Zr-2Mo (Ti-6242) are

used. β-alloys such as Ti-10V-2Fe-3Al (Ti-10-2-3) or the newer Ti-5Al-5V-5Mo-3Cr (Ti-5553) offer higher strength than Ti-6Al-4V and are used in e.g. landing gears [34].

3.2 Machinability of titanium alloys

The machinability of titanium alloys is severely impaired by a number of characteristics, such as their high specific strength kept at elevated temperatures, low thermal conductivity, low modulus of elasticity and chemical reactivity with most tool materials [36]. The strength at elevated temperatures leads to high cutting temperatures and stresses on the tool. Thermal conductivity in the order of 5 to 10 times lower than that of steel results in more heat being absorbed by the tool, and a much smaller proportion of heat being carried away by the chips. It is reported that the contact length between the chip and tool is short when machining titanium alloys. Consequently, the temperature gradient is steep and the high temperatures are found closer to the cutting edge [37]. Therefore, the application of coolant during the cutting process is important to minimize the tool wear.

4 Cryogenic machining

Although the cryogenic temperature range is commonly defined as temperatures lying below -150 °C or -180 °C [38], the term *cryogenic machining* has been used in a broader sense in reference to the use of a cooling medium at a temperature well below room temperature during some part of the machining process. This section provides a historical background and description of cryogenic machining, as well as some important results on cryogenic machining of titanium alloys from the literature.

4.1 Historical background

Research in the field of cryogenic machining was undertaken as early as the 1950's. The use of liquid carbon dioxide as a coolant in machining was described in 1953 by E.W. Bartle [39]. A rough-boring operation on a "high-nickel, high-chromium tungsten alloy steel" for a turbine nozzle box was carried out while liquid carbon dioxide was applied to the cutting edge of the tungsten carbide tool through a fine nozzle. The achieved cutting speed of 315 ft/min (96 m/min) and feed of 0.02 in/rev (0.5 mm/rev) was reported to have been a 100 % improvement over previously used cutting data for this workpiece material.

A cooling technique called CeDeCut, in which liquid CO_2 is directed at the leading edge of the tool through a capillary in the tool itself, was devised by the Carbon Dioxide Company. A description of the technique and some results were given in *Scientific Lubrication* in 1954 [40]. Tool life and cutting speed were both doubled compared to dry turning of high-tensile steel. Applications of CO_2 cooling in drilling and milling were also mentioned, as well as the combination of CO_2 and traditional cutting fluid. In 1955 [41], the CeDeCut technique was employed in the machining of Nimonic 95, a nickel alloy. By increasing the spindle rotational frequency from 106 r.p.m. to 180 r.p.m., the two machining stages required to manufacture a specific component were completed in 7.5 min where previously 12.75 min were needed. In 1965, L. Walter made a cost analysis of machining with and without CO_2 cooling using the CeDeCut technique [42]. He showed that on a per component basis, costs would be nearly cut by half with CO_2 cooling.

Hollis [43] described a cooling concept similar to CeDeCut in 1961: liquid carbon dioxide was injected into the tool holder through capillary tubing. The liquid CO_2 expanded to atmospheric pressure and CO_2 snow was deposited in a cavity under the tool tip.

Liquid nitrogen was used as early as 1958 to cool down the workpiece. Kumabe and Masuko [44] performed orthogonal cutting tests on mild steel, brass and duralumin and saw decreased cutting forces and surface roughness at lower temperatures.

The results of slotting tests on Ti-6Al-4V using a 5/8 in (15.875 mm) diameter end mill at 0.125 in (3.175 mm) depth of cut are given in [45]. The research was performed at Grumman Aircraft Engineering Corp. in 1965. Both liquid carbon dioxide and liquid nitrogen were evaluated as coolants compared to oil. At a cutting speed of 100 fpm (30 m/min), tool life increased from 70 in (1.78 m) of travel with oil coolant to 120 in (3.05 m) with liquid carbon dioxide (71 % increase) and 240 in (6.10 m) with liquid nitrogen (240 % increase).

The effects of cryogenic machining on carbon steel, stainless steel, and pure titanium were studied by Uehara and Kumagai in 1969 [46]. They used hollow workpieces that were internally cooled by liquid nitrogen flowing through tubing inserted in the spindle of the lathe. Uehara and Kumagai suggested that cryogenic cooling has a complex influence on the machining process. The cutting performance depended on both cutting conditions and the properties of the workpiece material. Notably, the cutting force decreased for carbon steel, which is subject to low temperature embrittlement, whereas it increased for stainless steel and titanium, which is not. The decrease in cutting force in turning carbon steel was more pronounced at low cutting speed.

The interest in cryogenic cooling seems to have faded from the early 1970's. However, the subject regained attention again in the early 1990's, notably with a series of publications by Hong et al. in the period 1992-2006 [47–57]. The number of published studies has sharply risen in recent years.

4.2 Cryogens and cryogen delivery methods

4.2.1 Cryogens

Liquid carbon dioxide (CO_2) and liquid nitrogen (LN_2) are the two coolants that are used in almost all studies related to cryogenic machining. Because of their differing properties, CO_2 and LN_2 require different methods of storing and handling. The respective phase diagrams are shown in figure 8. The liquefied gas is stored in a high-pressure tank. Liquid nitrogen is stored at low temperature in an insulated tank. When it is exposed to ambient pressure and temperature, the liquid nitrogen starts to boil at a temperature of -196 °C. In contrast, liquid carbon dioxide requires only high pressure and can be stored at room temperature. When released from its storage, the liquid carbon dioxide expands rapidly because of the large pressure drop and forms

a mixture of carbon dioxide snow ('dry ice') and gaseous CO_2 due to the Joule–Thomson effect. The CO_2-snow immediately sublimates at -78.5 °C.

Both with LN_2 and CO_2, the machined component is left residue-free after the process. Without the mist formation that is problematic when using conventional cutting fluids, the workshop environment is greatly improved. Nitrogen is the main constituent of air (about 78 % by volume) and is thus not toxic. However, vigilance is still required to avoid an increased concentration of nitrogen in a confined area, since lower concentration of oxygen can lead to suffocation. Carbon dioxide on the other hand is toxic in itself. In addition, CO_2 is heavier than air and accumulates close to the floor, whereas nitrogen is lighter than air.

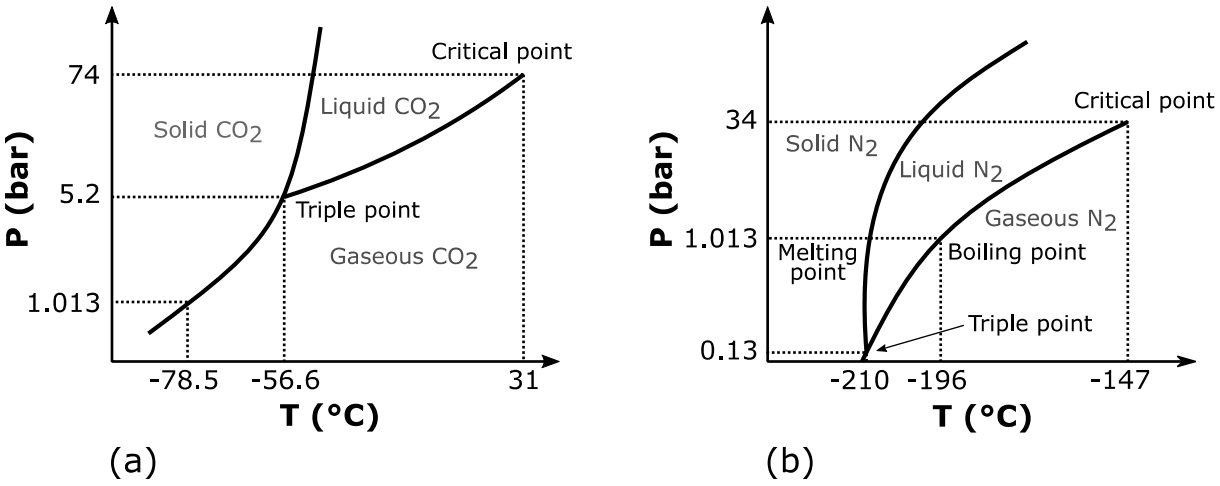

Figure 8: Phase diagrams of (a) carbon dioxide and (b) nitrogen. Adapted from [58].

4.2.2 Application of cryogenic coolants

A number of different strategies have been explored to take advantage of the cooling effect of cryogenic coolants. Gill et al. sought to improve the wear resistance of cutting tools by cryogenic treatment prior to the machining process [59]. Some researchers have applied the coolant to the workpiece, in order to change its material properties ahead of the cutting [46,49,60]. By means of specially designed tool holders, it is possible to cool the tool by circulating liquid nitrogen in a reservoir in contact with the tool. In this "indirect" approach, only the tool is cooled as no liquid nitrogen is sprayed on the workpiece [51,61]. In most studies on cryogenic machining, however, the adopted strategy is to apply the coolant to the cutting zone on the tool rake side, the tool flank side, or a combination thereof.

The supply of cryogenic coolant can be through external or internal/integrated nozzles. The strategy and setup used can have great influence on the results. In particular, the number of nozzles and their position [55,62], the flow rate of the coolant [63,64]-[paper 2 in this thesis] and the phase of the supplied coolant [65] are all important parameters to control.

Since CO_2 is stored in the liquid phase at room temperature, the pipes need only be pressure-resistant and no additional insulation is required [5]. This allows milling cutters to be design for delivery of CO_2 coolant through the spindle [66]-[papers 2 and 3 in this thesis]. LN_2 in contrast needs an insulated system and the low temperatures present a challenge for through spindle applications.

An interesting development is the combination of the cooling capabilities of cryogenic machining with the lubrication of MQL. Promising results have been reported when machining Ti-6Al-4V for the combination of CO_2+MQL in shoulder milling [67] and turning [68]. Similarly, lower flank wear was reported for the combination LN_2+MQL compared to LN_2 alone in turning Ti-6Al-4V [69].

4.3 Cryogenic machining of titanium alloys

Titanium alloys are among the most widely studied materials in the field of cryogenic machining. The α+β alloy Ti-6Al-4V, being the most common titanium alloy used in industry, features predominantly in the literature. The particular case of Ti-6Al-4V produced by additive manufacturing has recently been the object of intense focus by some researchers [70–76]. Other titanium alloys used in studies of cryogenic machining include the α+β alloy Ti-6Al-7Nb for biomedical applications [77] and β alloys Ti-10V-2Fe-3Al [78,79] and Ti-5553 [80].

4.3.1 Effects of cryogenic machining on tool wear and tool life

Longer tool life has been reported in many studies of cryogenic machining of Ti-6Al-4V compared to dry cutting or flood cooling with emulsion.

In their turning experiments on Ti-6Al-4V, Dhananchezian and Kumar [81] recorded a reduction of flank wear of 27-39 % with LN_2 cooling compared to emulsion cooling. Crater wear and flaking were also reduced by the cryogenic coolant. A reduction of the temperature in the heat generation zones led to less adhesion between the chip and the tool rake face.

Venugopal et al. studied the tool wear in turning of Ti-6Al-4V [82,83]. They reported that cryogenic cooling by liquid nitrogen was an effective way to slow the growth of tool wear. The tool life criteria of VB=0.3 mm at v_c=70 m/min (f=0.2 mm/rev) was reached after 24 min in

cryogenic machining, compared to 7 min for dry machining and 14 min with emulsion cooling. However, the improvement in tool life was not as significant at the higher cutting speeds tested (100 m/min and 117 m/min). The possible difficulty of the liquid nitrogen to penetrate the tool-chip interface at the higher cutting speeds was offered as an explanation. This highlights the importance of the setup for an efficient use of cryogenic cooling.

The significance of the coolant delivery system is also shown in two publication by Bermingham et al. [62,84]. In their turning experiments with LN_2, tool life is improved over dry cutting. More importantly, the relative increase in tool life greatly varied with the number and position of nozzles on the tool holder. Delivery of LN_2 to the flank in addition to the rake gave a longer tool life than cooling only the rake. Simultaneous cooling of the rake, flank and nose of the tool provided the longest tool life. Depending on cutting data, the improvement over dry cutting was 28-150 % [62]. In similar experiments, it was shown that wear was reduced where LN_2 was applied, i.e. abrasive wear on the flank was reduced and wear concentrated on the nose and rake when LN_2 was directed to the flank only [84].

While reporting increased tool life up to +20 % over emulsion cooling, Tirelli et al. [85] noted that improvement occurred mostly for low material removal rates and much less at higher cutting data. They concluded that cryogenic cooling with LN_2 may not be the best strategy for rough turning of Ti-6Al-4V.

Up to five times longer tool life was achieve by Krämer et al. with LN_2 compared to emulsion cooling (v_c=100 m/min, f=0.15 mm/rev, a_p=0.5 mm) [86]. In their turning experiments on Ti-6Al-4V, a comparison was made between LN_2 and CO_2 as coolant. The rate of flank wear development was higher with CO_2 than with LN_2 and highest with emulsion cooling.

Fewer results have been reported for cryogenic milling experiments of titanium alloys than cryogenic turning. In a study of end-milling with LN_2 cooling by an external nozzle, Shokrani et al. reported a three-fold increase in tool life over emulsion cooling [87]. Others have used a combination of cooled air and MQL with decreased tool wear as a result [88,89].

4.3.2 Effects of cryogenic machining on surface integrity

Much of the research on cryogenic machining has been focused on the potential improvements in terms of tool wear and tool life. Except for the surface roughness parameter Ra, which has been reported in many studies, less effort has so far been put into characterization of the surface integrity of titanium alloys after cryogenic machining.

In many cases, the reported values of Ra were lower in the case of cryogenic machining compared to emulsion cooling [61,77,81,90], dry cutting [77,91] or MQL [91]. The opposite, with cryogenic cooling producing rougher surfaces, has also been reported in some cases [73,92] for AM produced Ti-6Al-4V (EBM and DMLS).

In finish turning of Ti-6Al-7Nb, Sun et al. [77] measured significantly higher hardness on the surface after LN_2 cooling compared to dry and emulsion cooling (40.6 HRC vs. 30.4 HRC and 35.4 HRC respectively). The hardened layer was also deeper, reaching 1 mm below the surface. The increased hardness was attributed to the larger volume fraction of β phase that was measured in the affected layer after cryogenic cooling.

Similar results were reported for Ti-6Al-4V by Rotella et al. [91] with orthogonal cutting tests. Higher hardness was obtained when cooling with LN_2 than dry machining or using MQL. The difference was less apparent when changing the feed rate from f=0.1 mm/rev to f=0.05 mm/rev. In the former case, the higher hardness was also maintained deeper below the surface. There was also evidence of grain refinement produced by cryogenic cooling.

In the case of Ti-6Al-4V produced by electron beam melting (EBM), a comparison between micro-hardness profiles for different feed rates and lubrication strategies revealed no significant differences [92].

Sartori et al. [73] published residual stress profiles measured on AM produced Ti-6Al-4V after finish turning. Cryogenic cooling with LN_2 directed to the rake and flank faces was used, with dry cutting as a reference. The residual stresses were compressive in all cases but the stresses were higher and the affected layer was deeper with cryogenic cooling than after dry cutting.

In a set of turning experiments with different combinations of nozzle diameter and supply pressure of liquid nitrogen, producing different flow rates, Ayed et al. [64] reported that increasing the flow rate of LN_2 produced higher values of compressive stresses on the surface of the machined part. At constant flow rate, the combination of higher supply pressure (8-10 bar) and smaller nozzle diameter (2.5 mm) produced more compressive surface residual stresses than lower supply pressure (4-5 bar) combined with larger nozzle diameter (3 mm).

5 Experimental work

This section provides a description of the setups for the machining experiments as well as details on the analysis techniques used.

5.1 Cryogenic machining experiments

Two types of cryogenic machining experiments were conducted: longitudinal turning with cryogenic cooling using liquid nitrogen (LN_2) and face milling with cryogenic cooling using liquid carbon dioxide (CO_2). In all cases, the workpiece material was the α+β titanium alloy Ti-6Al-4V.

5.1.1 Cryogenic turning experiments with LN_2

Figure 9 shows the setup for the longitudinal turning experiments, which were conducted on a SMT Swedturn 12 lathe using cryogenic cooling with liquid nitrogen and flood-cooling with emulsion. The aim of these experiments was to study the influence of the cooling method and of the tool wear on the surface integrity of the machined workpieces (Paper 1). A prototype tool holder was used for all test conditions, enabling coolant delivery to the cutting zone through internal channels. The nozzle diameter was 0.4 mm and the flow was directed to the rake face of the tool. Liquid nitrogen was delivered at a pressure of 6.8 bar. The emulsion had a concentration of 6 % and was delivered at a pressure of 6 bar.

The influence of tool wear was studied by conducting the experiments with controlled flank wear (VB). A set of inserts with set levels of flank wear was made by turning a large bar of the same workpiece material until the desired level of VB was obtained. The inserts were commercially available uncoated cemented carbide inserts from Sandvik Coromant (VNMG 16 04 08-SM H13A). The cutting data is given in table 2 and a summary of test conditions is given in table 3.

Table 2: Cutting data (Paper 1)

Cutting data
v_c = 70 m/min
f = 0.15 mm/rev
a_p = 1.5 mm

Table 3: Test conditions for the longitudinal turning experiments (Paper 1)

Experiment	Cooling	Nominal VB_{max} [mm]
1	LN_2	New insert
2	LN_2	0.1
3	LN_2	0.2
4	LN_2	0.4
5	Emulsion	New insert
6	Emulsion	0.1
7	Emulsion	0.2
8	Emulsion	0.4

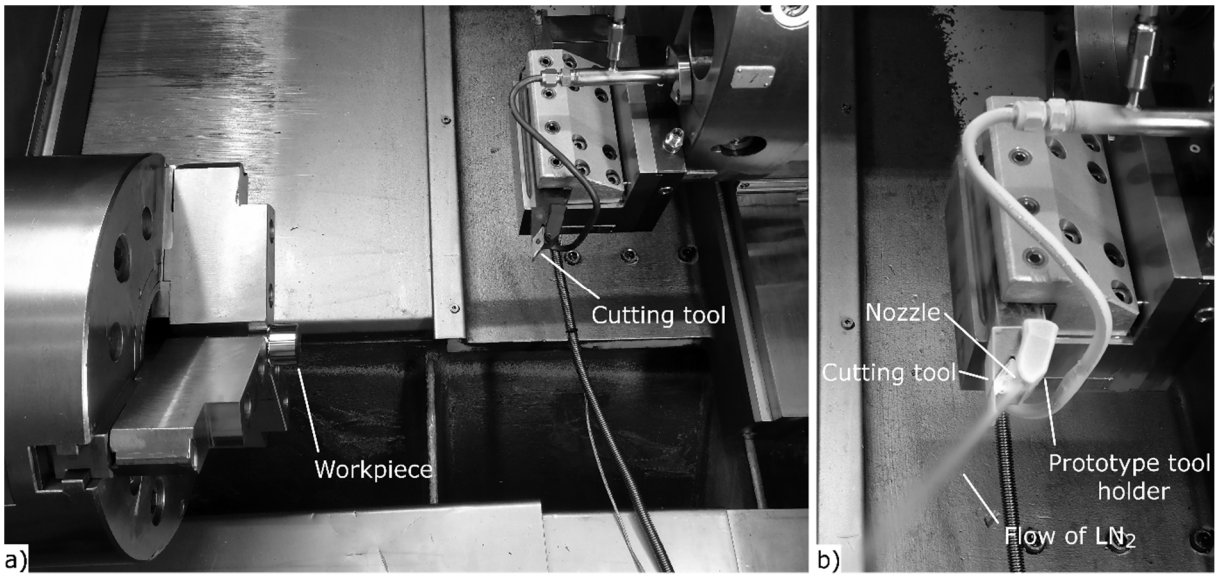

Figure 9: (a) Setup for longitudinal turning experiments. (b) Tool holder with cryogenic cooling activated.

5.1.2 Cryogenic milling experiments with CO_2

Face milling experiments were conducted on a Hermle C40U Dynamic machining centre. The cooling conditions were either cryogenic cooling using liquid carbon dioxide (CO_2) or flood-cooling with emulsion (Blasocut BC 25). The aim of these experiments was to study the tool life and wear development, as well as the wear mechanisms that determine tool life, under cryogenic cooling conditions compared to emulsion flood-cooling. In particular, the influence of the coolant flow rate (Paper 2) and of the PVD-coating vs. uncoated tools (Paper 3) was analyzed.

The cutter, CoroMill 600-040Q16-12H, was equipped with two inserts, each insert having an arc of engagement of 180°. The coolant was supplied through the machine spindle with a pressure of 50 bar for both cooling conditions. For the experiments presented in Paper 2, the standard cutter was redesigned in order to obtain varying flow rates of coolant using three different nozzle diameters. All tests were conducted using inserts of the same substrate and geometry. The coated inserts were grade 600-1252E-ML 1030, with a (Ti,Al)N coating. The uncoated inserts used in Paper 3 were grade 600-1252E-ML H13A. A summary of the test conditions for the face milling experiments is given in table 4.

Table 4: Summary of the test conditions for the face milling experiments.

	Paper 2	**Paper 3**
Cooling	CO_2 and emulsion Varying flow rate	CO_2 and emulsion Fixed flow rate
Inserts	600-1252E-ML 1030 (coated)	600-1252E-ML 1030 (coated) 600-1252E-ML H13A (uncoated)
Cutting data	v_c = 80 m/min fz = 0.15 mm/tooth a_p = 2 mm	v_c = 60-100 m/min fz = 0.1-0.2 mm/tooth a_p = 2 mm

5.2 Analysis techniques

5.2.1 Residual stress measurements by X-ray diffraction

When X-rays are directed onto a sample, the atoms of the sample material scatter the X-rays in all directions. In crystalline materials, where atoms are arranged in regular arrays, scattered X-rays are produced in regular arrays of spherical waves. However, in most directions, the waves of the scattered radiation cancel each other out due to destructive interference. In some specific directions, constructive interference can occur, creating a diffracted beam of X-rays. The conditions in which coherent scattering of the X-rays from the crystal lattice of the sample occurs are given by Bragg's law given in eq. (1):

$$n\lambda = 2d\,sin\theta \tag{1}$$

where n is a positive integer, λ is the wavelength of the incident X-ray, d is the interplanar spacing in the crystal lattice, and θ is the scattering angle [93]. In order for constructive interference to occur, the difference in path length between two scattered beams must be a multiple of the wavelength of the radiation, as illustrated in figure 10.

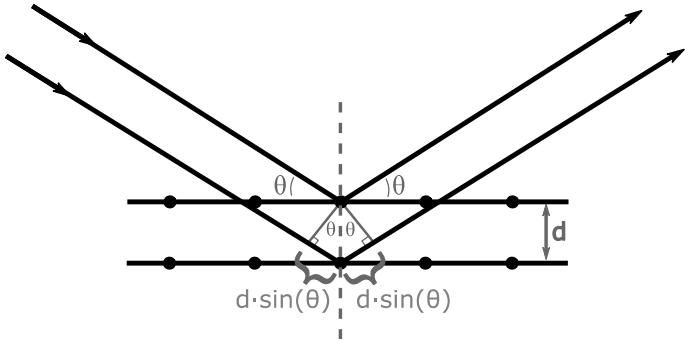

Figure 10: Diffraction of X-rays in a crystal. The figure shows the scattering angle θ and the interplanar spacing d. The difference in path length between two scattered beams is 2d·sin(θ). Constructive interference occurs if this difference in path length is a multiple of the wavelength of the incident X-rays.

For a given X-ray wavelength and diffraction angle, the interplanar spacing of the crystal lattice of an unstrained material will produce a diffraction pattern that is characteristic for that material. When the material is strained, the interplanar spacing is changed, either bringing the lattice planes of the crystal closer to each other or farther apart. As a result, there will be a shift in the diffraction pattern. X-ray diffraction is thus not used to directly measure the stress state in a material: the strains are deduced from the precise measurement of the shift in the diffraction pattern; stresses can then be calculated from the general form of Hooke's Law [30,94].

Figure 11 shows a schematic representation of a portion of the sample surface. Since the measurement is made at the surface, the stress state is assumed to be biaxial (plane stress condition) and the stress component perpendicular to the surface σ_3 is equal to zero. The principal stress components σ_1 and σ_2 are lying within the surface plane.

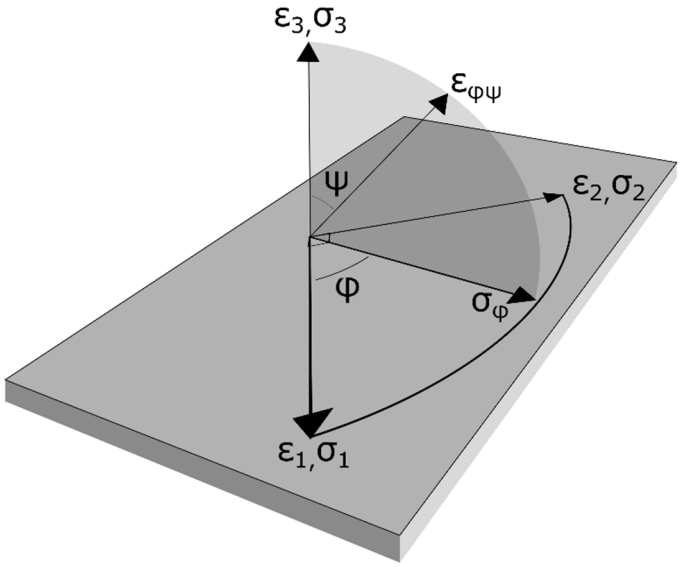

Figure 11: Principal stresses and corresponding strains. The stress direction of interest is σ_φ. Plane stress condition is assumed so that $\sigma_3=0$.

Unlike σ_3, the strain normal to the surface, ε_3, is not zero. The corresponding interplanar spacing is measured directly by solving equation (1) for d_n. The strain is then given by:

$$\varepsilon_3 = \frac{d_n - d_0}{d_0} \tag{2}$$

where d_0 is the unstrained interplanar spacing. In the same way, the interplanar spacing in the $\varphi\psi$-direction can be measured by tilting the incident-ray beam, thus giving the corresponding strain:

$$\varepsilon_{\varphi\psi} = \frac{d_{\varphi\psi} - d_0}{d_0} \tag{3}$$

The strain along the $\varphi\psi$-direction can be expressed as:

$$\varepsilon_{\varphi\psi} = \frac{d_{\varphi\psi} - d_0}{d_0} = \frac{1+\nu}{E}\sigma_\varphi \sin^2\psi - \frac{\nu}{E}(\sigma_1 + \sigma_2) \quad (4)$$

where E and ν are the modulus of elasticity and the Poisson's ratio of the sample material [30]. Rearranging equation (4) provides the relationship between the interplanar spacing and the biaxial stresses present in the surface of the material:

$$d_{\varphi\psi} = \frac{1+\nu}{E}\sigma_\varphi\, d_0 \sin^2\psi - \frac{\nu}{E} d_0(\sigma_1 + \sigma_2) + d_0 \quad (5)$$

Equation (5) shows a linear relationship between the interplanar spacing $d_{\varphi\psi}$ and $\sin^2\psi$. If a number of measurements are made at different tilt angles ψ, the surface stress σ_φ can be obtained by calculating the slope of a line fitted to the experimental data. Differentiating equation (5) with respect to $\sin^2\psi$ gives the slope m, from which σ_φ can be solved:

$$m = \frac{\partial d_{\varphi\psi}}{\partial \sin^2\psi} = \frac{1+\nu}{E}\sigma_\varphi d_0 \quad (6)$$

$$\sigma_\varphi = \left(\frac{E}{1+\nu}\right)\frac{1}{d_0} m \quad (7)$$

Computing σ_φ from equation (7) requires knowledge of the unstrained interplanar spacing d_0. However, the lattice spacing measured at $\psi = 0$ can be substituted for d_0 with an error of less than 1 %, rendering *a priori* knowledge of d_0 unnecessary for practical applications [95]. This procedure, where multiple ψ-tilts are used to find the stress σ_φ is commonly known as the "$\sin^2\psi$" technique.

In this work, the residual stress measurements were performed on an Xstress 3000 G2R diffractometer with a Ti-Kα radiation. The $\sin^2\psi$ method was used, with measures done at 5 tilts each for positive and negative ψ angles from 0° to ±40°, with equal intervals in $\sin^2\psi$. Stresses were calculated using the diffraction peak for the {110} family of planes with a Bragg angle 2θ = 137.4° (see figure 6 in section 3 for an illustration of the plane in the unit cell of the α phase). The elastic modulus was set to 120 GPa and Poisson's ratio to 0.36. The diffraction patterns were analyzed in the XTronic V1.9 software and the position and intensity of the peaks were determined by fitting of the Pearson VII function with parabolic background. The residual stresses were determined in the hoop and axial directions, corresponding to the direction of cut and feed, as illustrated in figure 12.

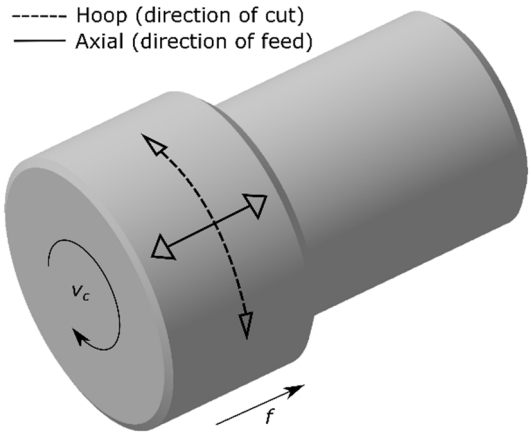

Figure 12: Schematic representation of the hoop and axial directions of the measured residual stresses on the machined surface.

Due to absorption, the incident X-ray beam is attenuated as it passes through the sample material. As a consequence, diffraction occurs only from a thin layer of material close to the sample surface. The diffracted intensity also varies with depth, since a longer path to travel within the material leads to stronger attenuation, and the diffracted beam is in turn attenuated as it exits the material. The penetration depth of the X-rays can be defined in terms of the fraction of the total diffracted intensity that originates from within that depth. Defined as the depth x out of which 63 % of the diffracted intensity originates, the penetration depth is given by the expression [96]:

$$x = \frac{1}{2\mu} \sin\theta \cos\psi \tag{8}$$

where μ is the attenuation coefficient. With μ = 513 cm^{-1} [96], the penetration depth of Ti-Kα radiation into titanium for the {110} peak at 2θ = 137.4° is thus approximately 6.5 μm to 9 μm for ψ-tilt angles of 0° to 45°.

The depth of penetration of X-rays being limited to the first few micrometers, it is necessary to remove layers of material in order to determine the residual stress distribution as a function of depth into the sample. Any mechanical method will deform the surface and thus alter the stress state of the sample, regardless of how fine the grinding or polishing. Electrolytic polishing, on the other hand, provides a deformation free surface and is therefore the preferred method of layer removal for measuring residual stress profiles [95]. Electropolishing is an electrochemical process: the metallic sample is made into an anode by connecting it to the positive terminal of a direct current power supply. It is exposed to (sometimes immerged in) an electrolyte. A cathode, immerged in the electrolyte, is connected to the negative terminal of the power supply.

When a voltage is applied, current is created in this electrolytic cell. If an appropriate voltage is chosen, controlled dissolution of the anode material occurs [97].

A Struers LoctroPol-5 electrolytic polishing machine was used for layer removal in this work. The chemical composition of the electrolyte used (Struers Electrolyte A3) is given in table 5. The depth of material removed was measured after each electropolishing step by a stylus profilometer. Figure 13 shows the surfaces obtained at two different stages of material removal.

Table 5: Chemical composition of Struers Electrolyte A3.

1 part	**16 parts**
Perchloric acid (60 % concentration)	Methanol (55-75 %) 2-butoxyethanol (25-45 %)

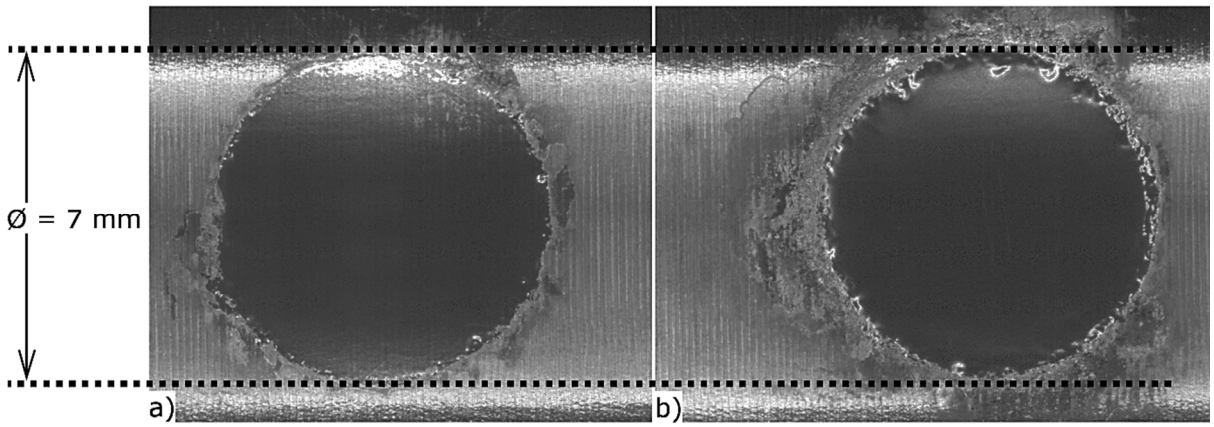

Figure 13: Micrographs of the surfaces obtained after layer removal by electropolishing. The two images show the same sample at different stages of material removal: (a) 12 μm and (b) 110 μm.

5.2.2 Surface roughness measurements

The surface roughness of the turned samples was evaluated by a Somicronic Surfascan profilometer. Gaussian filtering was applied with a cut-off length of $\lambda = 0.8$ mm. The measurements were made at regular intervals around the machined surface, in the direction of feed.

5.2.3 Tool wear evaluation

The development of tool wear was monitored using an optical microscope (Nikon SMZ1000) equipped with software for tool wear measurement. The tool life criteria in Papers 2 and 3 were set according to ISO 8688 [98] to VB = 0.3 mm for flank wear and $VB_N = 0.4$ mm for notch wear. A maximum of 300 min cutting time was allowed if the tool life criteria were not met. The worn inserts were then examined in a Zeiss SUPRA 40 Scanning Electron Microscope.

5.2.4 Microstructural characterization

The turned samples were sectioned, mounted and prepared for microstructural characterization. Sectioning was performed using a Struers Discotom-2 cut-off machine with 20S25 cut-off wheels and the samples were hot mounted in Struers PolyFast mounting resin. The orientation of sectioning and mounting is illustrated in figure 14. All grinding and polishing steps were performed on a Struers TegraPol-31/TegraForce-5 polishing machine. Plane grinding was done using P320 SiC paper, followed by fine grinding on a MD-Largo disc with a 9 μm diamond suspension. A MD-Chem cloth with OP-S solution was used for the final polishing step. The microstructure was revealed using Kroll's etchant (see chemical composition in table 6).

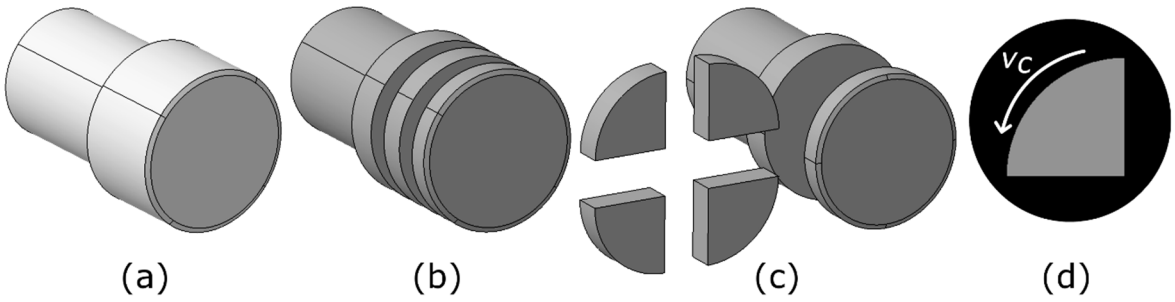

Figure 14: Schematic illustration of the sectioning and mounting of samples for microstructural characterization. (a) Machined sample. (b)-(c) Sectioning steps. (d) Top view of mounted sample.

Table 6: Chemical composition of Kroll's etchant used for revealing the microstructure in titanium alloy Ti-6Al-4V.

Water	**HNO_3**	**HF**
100 ml	20 ml (65 % conc.)	10 ml (40 % conc.)

6 Summary of results and discussion

6.1 Surface integrity in cryogenic turning with liquid nitrogen (Paper 1)

The influence of cryogenic cooling with liquid nitrogen on the surface integrity was investigated in Paper 1. Surface roughness, residual stresses and the microstructure of the machined workpieces were studied at different levels of flank wear (new insert, VB=0.1 mm, VB=0.2 mm and VB=0.4 mm). The results obtained with cryogenic cooling were compared to those obtained with emulsion cooling using otherwise identical setups: same cutting data (v_c=70 m/min, f=0.15 mm/rev and a_p=1.5 mm), same nozzle size (0.4 mm diameter) and comparable coolant supply pressure (6.8 bar and 6 bar for liquid nitrogen and emulsion respectively).

It was found that the surface integrity, in terms of residual stresses, microstructure and surface roughness, was not significantly affected by the change of coolant nature from emulsion to LN_2. The residual stresses were measured in the direction of cut (hoop) and in the direction of feed (axial). As shown in the depth profiles presented in figure 15, the residual stresses were compressive with all combinations of coolant and level of flank wear.

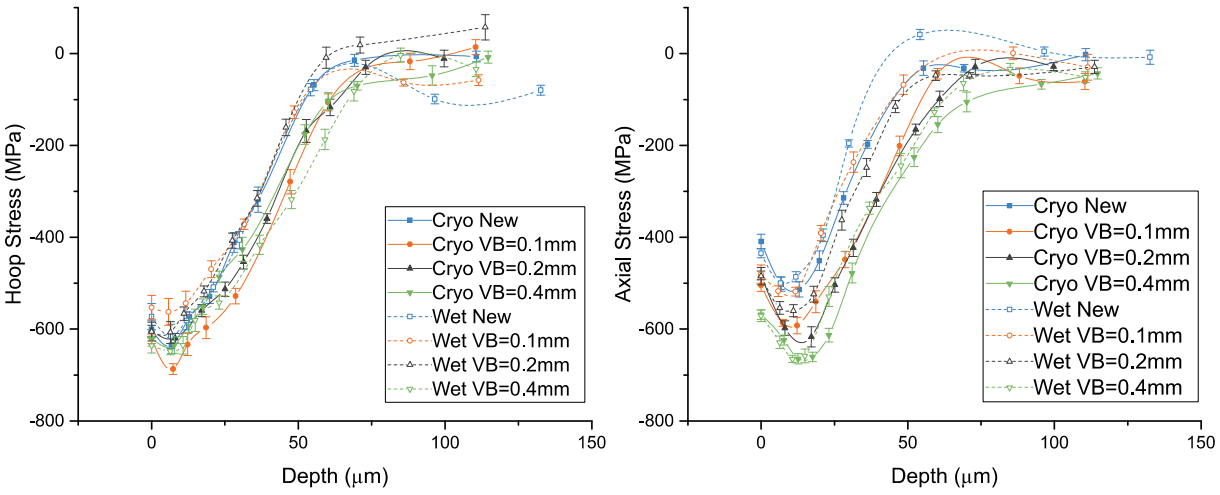

Figure 15: Residual stress profiles in the hoop (left) and axial (right) directions for all combinations of coolant and level of flank wear.

The residual stresses differ between the hoop and axial directions. The magnitude of the compressive residual stresses on the surface is higher in the hoop direction than in the axial direction. In both cryogenic and flood cooling conditions, the values differ by approximately 120 MPa for new inserts and 40 MPa for the severely worn inserts (VB=0.4 mm). The shape of the residual stress profiles also differ: whereas the residual stresses in the axial direction have

a distinct “hook” shape, with a clear dip at some distance from the surface, this dip is less clearly apparent in the hoop direction.

Considering especially the stresses in the axial direction, the profiles had a similar shape for all levels of flank wear but increasing the flank wear shifted the profiles towards higher compressive residual stresses. This trend was apparent in both cooling conditions, as seen in figure 16.

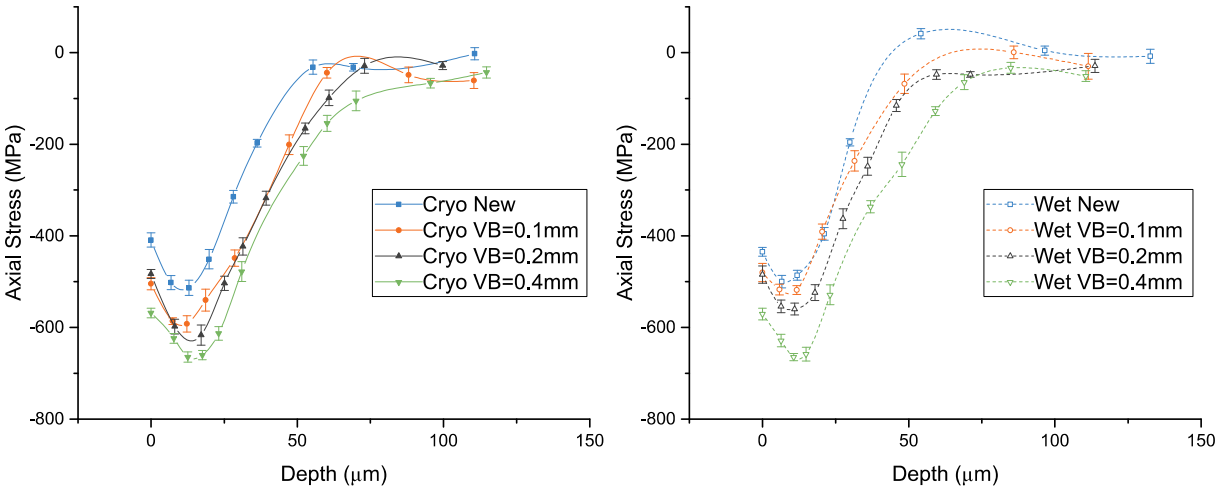

Figure 16: Residual stress profiles in the axial direction for cryogenic cooling (left) and flood emulsion cooling (right).

A comparison between the stress profiles for cryogenic and emulsion cooling at similar levels of flank wear reveals that for new inserts and for VB=0.4 mm, the cooling conditions had very little impact on the residual stress levels. For the intermediate levels of flank wear, the residual stresses are of the same magnitude at the surface but differ below the surface (figure 17).

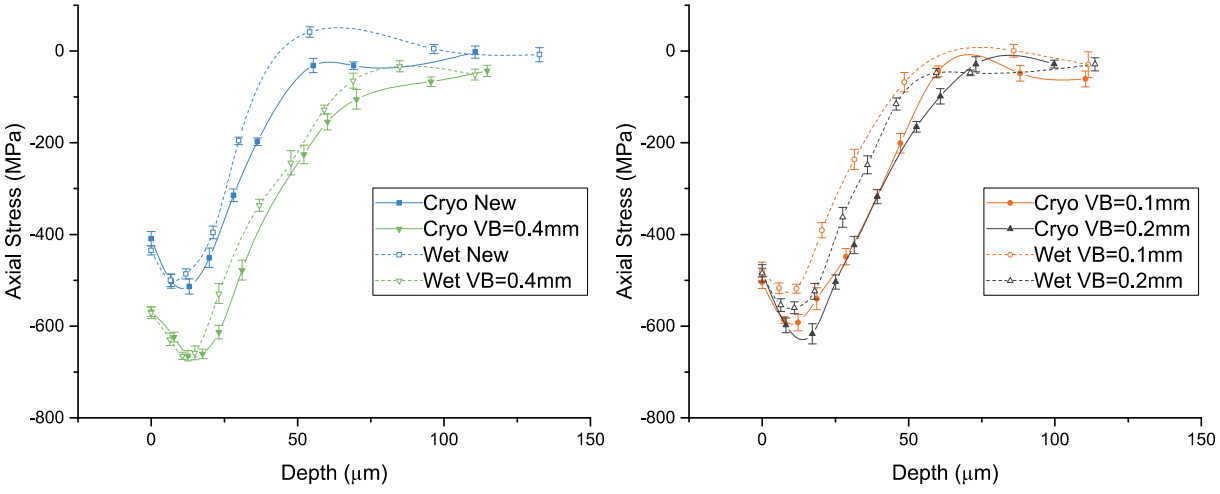

Figure 17: Residual stress profiles in the axial direction for new inserts and VB=0.4 mm (left); VB=0.1 mm and VB=0.2 mm (right).

The results in figures 15 to 17 show that maximum compressive residual stresses were measured at approximately 10 to 12 µm below the surface. The magnitude of the residual stresses then decrease monotonically with increasing depth. It can be seen that the depth of the affected zone ranges from 55 µm to 75 µm.

The broadening of the diffraction peaks obtained from the XRD measurements, as measured by their full width at half maximum (FWHM), is often used as an indicator of cold work or plastic deformation. FWHM profiles in the hoop and axial directions are presented in figure 18, showing an affected zone depth of 50-60 µm. The FWHM values are high near the surface and decrease sharply until stabilizing below this depth. The FWHM profiles are similar for all combinations of coolant and flank wear tested.

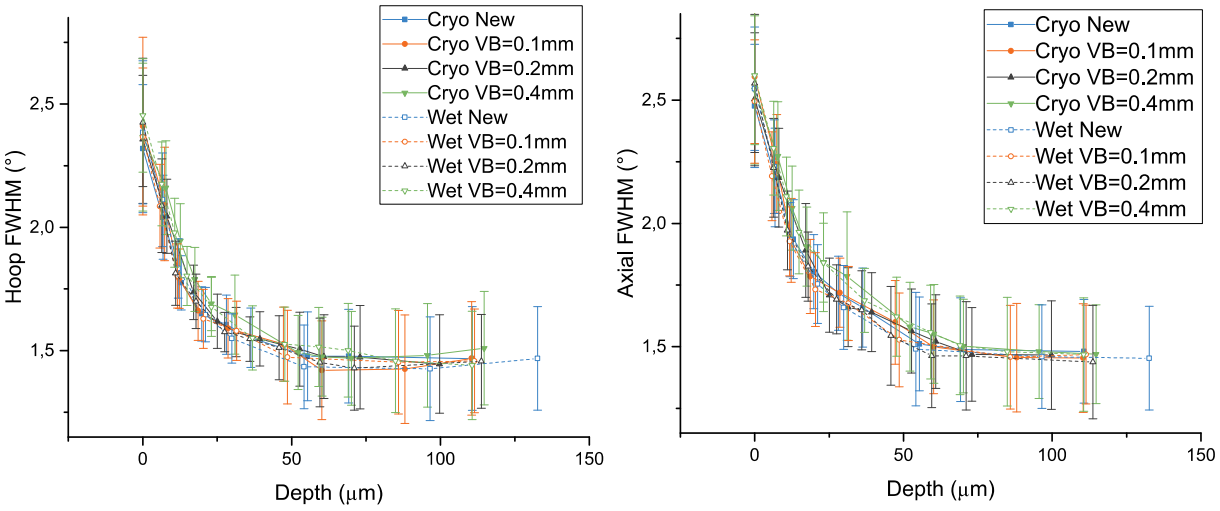

Figure 18: Full width at half maximum (FWHM) of the diffraction peaks obtained in the hoop (left) and axial (right) directions.

The microstructure of the machined workpieces was studied in cross sections parallel to the direction of cut. Figure 19 shows that the microstructure obtained after machining presents similar characteristics in all cutting conditions. The surfaces show no signs of fracture or cracks. A deformed layer is clearly visible, with a depth of approximately 10 µm, which corresponds to the depth at which the maximum compressive residual stresses have been measured. The residual stress and FWHM profiles thus indicate a deeper affected layer (~50-75 µm) than is observed in the microstructure. Of course the FWHM values are highest near the surface and rapidly decrease: plastic deformation occurs closest to the surface.

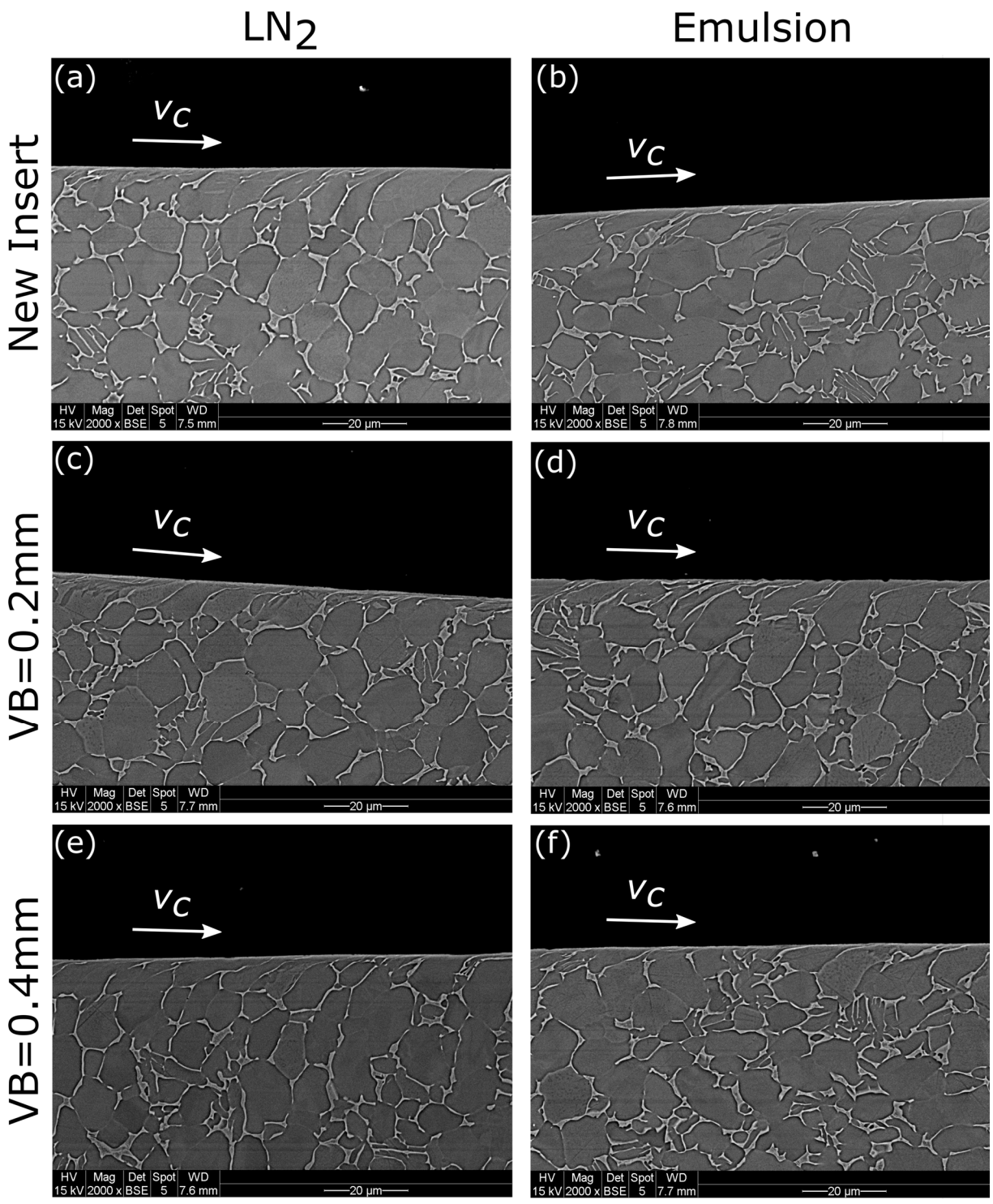

Figure 19: SEM images of cross sections of the machined workpieces for different combinations of coolant and level of flank wear.

The similarity between the results obtained with cryogenic cooling and flood cooling is important in light of the small nozzle size for coolant supply used in these experiments. The machining times required to obtain the different levels of flank wear used in this experiment are given in table 7.

Table 7: Machining times to obtain the desired levels of flank wear.

Nominal VBmax [mm]	Cryogenic LN_2	Flood emulsion
0.1	3 min	10 min
0.2	9 min	19 min
0.4	12 min	27.5 min

The limited flow rate of cryogenic coolant clearly had a negative impact on the rate of tool wear development. Yet, the surface integrity was not significantly affected in terms of residual stresses, microstructure and surface roughness. This suggests that an optimum balance between the consumption of cryogenic coolant, tool life and obtainable surface integrity could be found with careful setup of the coolant supply.

6.2 Cryogenic face milling with liquid carbon dioxide (Papers 2 and 3)

6.2.1 Tool wear development and wear mechanisms

The wear development and wear mechanisms were studied for face milling of Ti-6Al-4V, using both cryogenic cooling (liquid carbon dioxide) and flood cooling (emulsion). Irrespective of the flow rate of the coolant (Paper 2) and whether using coated or uncoated tools (Paper 3), it was found that abrasive wear, in the form of flank wear, is not the wear mechanism determining tool life. This was observed both when using liquid carbon dioxide and emulsion as a coolant. Instead, the main type of tool wear governing the tool life performance was notch wear or chipping/partial destruction of the cutting edge.

In the experiments presented in Paper 2 (cutting data: v_c=80 m/min, f_z=0.15 mm/tooth, a_p= 2mm), the development of flank wear was slower in the cryogenic cooling condition compared to flood cooling with emulsion. However, the tool life criterion for flank wear (VB=0.3 mm) was not met in either case. The flow rate of the coolant had limited effect on the development of flank wear, but clearly affected the development of notch wear. Notably, in the case of cryogenic cooling, each increase in flow rate delayed the appearance of notch wear, as shown in figure 20.

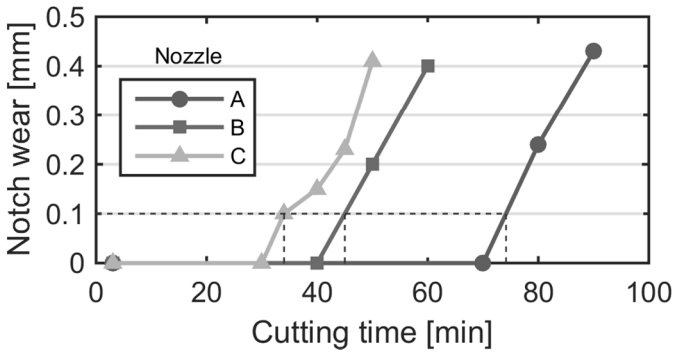

Figure 20: Notch wear development as a function of cutting time with liquid carbon dioxide cooling (Paper 2). Nozzles A had the largest diameter and nozzle C the smallest.

Analysis of the worn inserts by SEM reveals an important difference in the wear mechanism at play when comparing the two cooling conditions. Thermal fatigue cracks, also referred to as comb cracks, can be seen in both cases. These cracks are commonly found as a result of the cyclic thermal stresses due to the intermittent nature of the milling process and are oriented perpendicular to the cutting edge. When emulsion cooling is used, lateral cracks are also apparent. As these lateral cracks propagate and meet the comb cracks, part of the cutting edge is removed. The cutting edges of the tools used with cryogenic cooling are thus characterized by clearly defined and evenly spaced comb cracks. With emulsion cooling, in contrast, the cutting edges are characterized by more severe chipping. The difference in crack formation between cryogenic and emulsion cooling is shown in figure 21.

The difference in wear mechanisms was attributed to the CO_2 providing a uniform and rapid cooling over the contact area between the chip and tool. Up to moderate cutting data, the CO_2 is better able to penetrate the cutting zone than emulsion to dissipate heat. Increasing the flow rate of CO_2 further reduced the thermal stress, delaying the lateral propagation of cracks.

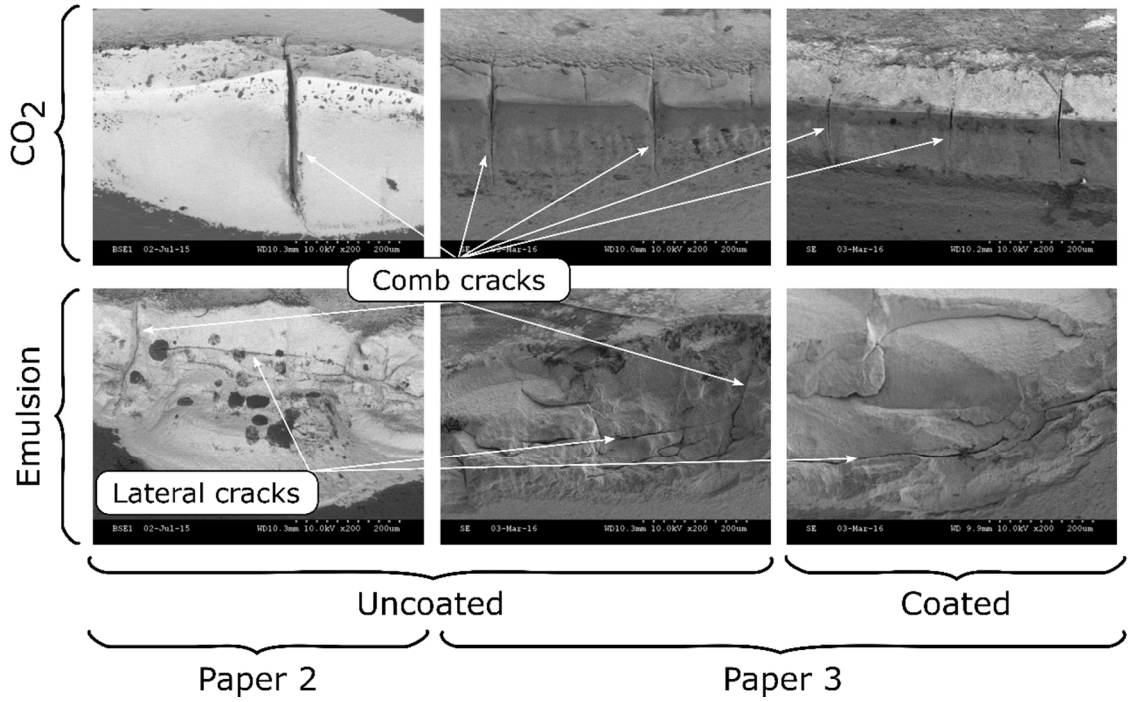

Figure 21: Cracks formed on the tool cutting edge when face milling Ti-6Al-4V. The cutting data in all cases was: v_c=80 m/min, f_z=0.15 mm/tooth and a_p=2 mm.

Figure 21 also shows that the same pattern occurs whether the tools are coated or uncoated, as found in paper 3. The type of crack and the direction of crack propagation is clearly determined by the choice of coolant.

6.2.2 Tool life performance

The experiments analyzed in Paper 2 and Paper 3 show how the achievable tool life when face milling Ti-6Al-4V is affected by: (1) the choice of coolant, (2) the flow rate of the coolant, (3) the choice of uncoated or coated inserts, and (4) the choice of cutting data. Several conclusions can be drawn. The cryogenic coolant CO_2 can drastically improve the tool life compared to emulsion flood-cooling. However, the effect of the cryogenic coolant on the tool life is dependent on the cutting data. As illustrated in figure 22, cryogenic cooling can provide up to 6 times increase in tool life compare to emulsion cooling (with uncoated tools at v_c=80 m/min and f=0.1 mm/tooth). As the cutting data increases, the difference in tool life obtained between cryogenic and emulsion flood-cooling decreases. At the highest combinations of cutting speed and feed, the difference is entirely eliminated.

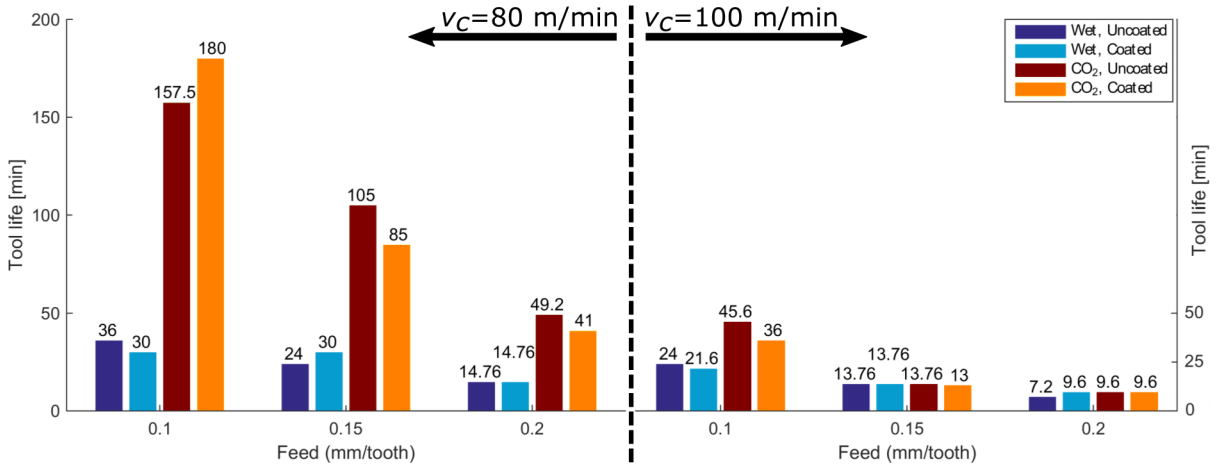

Figure 22: Tool life obtained for different combinations of cutting data, coolant and tool. (Paper 3)

Figure 22 also shows that using coated tools does not offer any improvement in tool life in either cooling condition.

Significant improvement in tool life with cryogenic cooling, up to 4.5 times longer than with emulsion, is also shown in figure 23 for moderate cutting data (v_c=80 m/min and f=0.1 mm/tooth). Here, the influence of the flow rate of CO_2 is evident: the tool life increases from 50 to 90 minutes (+ 80 %) between the lowest and highest flow rate. The corresponding tool life increase for flood cooling was from 16 to 20 minutes (+ 25 %).

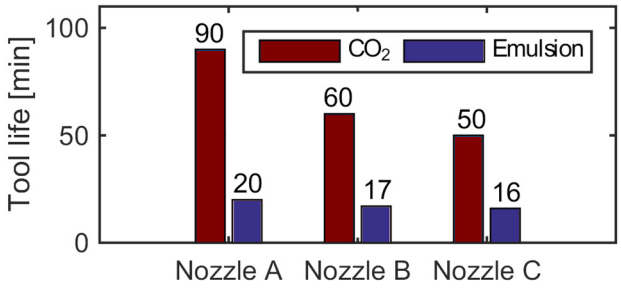

Figure 23: Tool life obtained using 3 different nozzle sizes A>B>C. Cutting data: v_c=80 m/min, f=0.15 mm/tooth, a_p=2 mm. (Paper 2)

6.3 Concluding remarks

Cryogenic cooling can be applied to machining processes with different goals in mind. Technical and economic objectives include improved machinability and prolonged tool life, leading to lower production costs. Achieving the desired levels of surface integrity, ensuring the functional performance of the machined parts, is also paramount. Removing oil-based coolants from the machining process and replacing them with clean cryogens meets

environmental and ecological objectives. The working environment in the workshop is improved and the production and disposal of oil-based cutting fluids is avoided.

The results presented in Papers 1-3 point to the potential of cryogenic cooling to meet these objectives. However, it is important to note that the goals have to be clearly defined. Finding the correct combination of cryogenic cooling setup with an appropriate window of cutting data for each intended application is necessary to fully take advantage of the potential of cryogenic cooling.

7 Future work

The results presented in Paper 1 suggest that an optimum balance between the consumption of cryogenic coolant, tool life and surface integrity can be obtained with an appropriate setup of the coolant supply. The response, in terms of tool life and surface integrity, to variations in the coolant supply parameters should be further investigated. Moreover, it would be useful to extend the testing to cover a range of relevant cutting data for finishing operations.

The surface integrity characterization should be expanded to include hardness profiles. X-ray diffraction (XRD) can be used to evaluate if phase changes have occurred, as well as the ratio of phases present in the surface layer. It would also be interesting to relate the tested parameters (choice of coolant, coolant supply conditions, cutting data, tool wear) to fatigue life.

Careful evaluation of the temperature in the cutting zone would provide valuable insights to determine the influence of thermal loads on the surface integrity, as well as important data for modelling and simulation purposes. Advanced characterization techniques, such as electron backscatter diffraction (EBSD) and transmission electron microscopy (TEM), could provide a deeper understanding of the deformation mechanisms in the near-surface layer.

The results point to a lack of lubrication when turning Ti-6Al-4V with liquid nitrogen as a coolant. Combining the cooling capability of liquid nitrogen with a minimum quantity lubrication (MQL) system could reduce the friction on the tool and thus increase tool life.

Acknowledgements

I would like to express my gratitude to Adj. Prof. Ibrahim Sadik for his guidance and patience. Thanks to Prof. Lars Nyborg for giving me the opportunity to join the department of Industrial and Materials Science (then department of Materials and Manufacturing Technology). Thanks to Prof. Peter Krajnik for support, encouragement and constructive feedback. Many thanks to Dr. Amir Malakizadi for being generous with his time, sharing his wisdom and contributing to a friendly atmosphere. Special thanks to Prof. Uta Klement for encouragement and support.

Thanks to all colleagues at the department of Industrial and Materials Science for providing a friendly working environment. Thanks to Roger Sagdahl, Dr. Yiming Yao and Dr. Eric Tam for practical help with microscopy, sample preparation and residual stress measurements. Thanks to Dinesh Mallipeddi, Sakari Tolvanen and Philipp Hoier for discussions about residual stresses, titanium and machining.

Thanks to Tommy Köhl and Johan Sternheden at Sandvik Coromant for help with experiments and data analysis. Thanks also to Jonas Holmberg at Swerea IVF for discussions about residual stresses.

Thanks to friends and family, near and far. Last but not least, my deepest gratitude goes to Joraine for her unwavering support, and to our newborn daughter Solveig, who is already a great teacher.

References

[1] World Commission on Environment and Development. Our Common Future, Oxford University Press, Oxford - New York, 1987.

[2] UN General Assembly. Resolution 70/1, Transforming our world : the 2030 Agenda for Sustainable Development, A/RES/70/1 (25 September 2015). Available at undocs.org/A/RES/70/1 .

[3] A.D. Jayal, F. Badurdeen, O.W. Dillon, I.S. Jawahir. Sustainable Manufacturing: Modeling and Optimization Challenges at the Product, Process and System Levels. CIRP J. Manuf. Sci. Technol. 2010; 2 (3): 144–152.

[4] F. Pušavec, P. Krajnik, J. Kopac. Transitioning to Sustainable Production – Part I: Application on Machining Technologies. J. Clean. Prod. 2010; 18 (2): 174–184.

[5] I.S. Jawahir, H. Attia, D. Biermann, J. Duflou, F. Klocke, D. Meyer, S.T. Newman, F. Pušavec, M. Putz, J. Rech, V. Schulze, D. Umbrello. Cryogenic Manufacturing Processes. CIRP Ann. - Manuf. Technol. 2016; 65 (2): 713–736.

[6] E.O. Ezugwu, J. Bonney, Y. Yamane. An Overview of the Machinability of Aeroengine Alloys. J. Mater. Process. Technol. 2003; 133: 233–253.

[7] E.M. Trent, P.K. Wright. Metal Cutting, 4th ed., Butterworth-Heinemann, Boston, 2000.

[8] F. Klocke. Manufacturing Processes 1, Springer-Verlag, Berlin Heidelberg, 2011.

[9] W. Grzesik. Advanced Machining Processes of Metallic Materials - Theory, Modelling and Applications., Elsevier, 2008.

[10] G.T. Smith. Cutting Tool Technology, Springer-Verlag, London, 2008.

[11] S. Debnath, M.M. Reddy, Q.S. Yi. Environmental Friendly Cutting Fluids and Cooling Techniques in Machining: A Review. J. Clean. Prod. 2014; 83: 33–47.

[12] M.A. El Baradie. Cutting Fluids: Part I. Characterisation. J. Mater. Process. Technol. 1996; 56 (1–4): 786–797.

[13] M.C. Shaw. Metal Cutting Principles, 2nd ed., Oxford University Press, New York, 2005.

[14] Y. Yue, J. Sun, K.L. Gunter, D.J. Michalek, J.W. Sutherland. Character and Behavior of Mist Generated by Application of Cutting Fluid to a Rotating Cylindrical Workpiece, Part 1: Model Development. J. Manuf. Sci. Eng. 2004; 126 (3): 417–425.

[15] R. M'Saoubi, D. Axinte, S.L. Soo, C. Nobel, H. Attia, G. Kappmeyer, S. Engin, W.-M. Sim. High Performance Cutting of Advanced Aerospace Alloys and Composite Materials. CIRP Ann. - Manuf. Technol. 2015; 64 (2): 557–580.

[16] C. Courbon, D. Kramar, P. Krajnik, F. Pusavec, J. Rech, J. Kopac. Investigation of Machining Performance in High-Pressure Jet Assisted Turning of Inconel 718: An Experimental Study. Int. J. Mach. Tools Manuf. 2009; 49 (14): 1114–1125.

[17] A.K. Nandy, M.C. Gowrishankar, S. Paul. Some Studies on High-Pressure Cooling in Turning of Ti–6Al–4V. Int. J. Mach. Tools Manuf. 2009; 49 (2): 182–198.

[18] E.O. Ezugwu, R.B. Da Silva, J. Bonney, Á.R. Machado. Evaluation of the Performance

of CBN Tools When Turning Ti–6Al–4V Alloy with High Pressure Coolant Supplies. Int. J. Mach. Tools Manuf. 2005; 45 (9): 1009–1014.

[19] K. Weinert, I. Inasaki, J.W. Sutherland, T. Wakabayashi. Dry Machining and Minimum Quantity Lubrication. CIRP Ann. 2004; 53 (2): 511–537.

[20] B. Davis, J.K. Schueller, Y. Huang. Study of Ionic Liquid as Effective Additive for Minimum Quantity Lubrication during Titanium Machining. Manuf. Lett. 2015; 5: 1–6.

[21] S. Sartori, A. Ghiotti, S. Bruschi. Solid Lubricant-Assisted Minimum Quantity Lubrication and Cooling Strategies to Improve Ti6Al4V Machinability in Finishing Turning. Tribol. Int. 2018; 118: 287–294.

[22] S. Pervaiz, A. Rashid, I. Deiab, C.M. Nicolescu. An Experimental Investigation on Effect of Minimum Quantity Cooling Lubrication (MQCL) in Machining Titanium Alloy (Ti6Al4V). Int. J. Adv. Manuf. Technol. 2016; 87 (5–8): 1371–1386.

[23] M.I. Sadik. An introduction to cutting tools - materials and applications, 2nd ed., Sandvik Coromant, 2015.

[24] A.C. a. De Melo, J.C.G. Milan, M.B. Da Silva, Á.R. Machado. Some Observations on Wear and Damages in Cemented Carbide Tools. J. Brazilian Soc. Mech. Sci. Eng. 2006; 28 (3): 269–277.

[25] M. Field, J.F. Kahles. The Surface Integrity of Machined and Ground High Strength Steels. DMIC Rep. 210 1964; 54–77.

[26] M. Field, J.F. Kahles, J.T. Cammett. Review of Measuring Methods for Surface Integrity. Ann CIRP 1972; 21 (2): 219–238.

[27] R. M'Saoubi;, J.C. Outeiro, H. Chandrasekaran, O.W.D. Jr., I.S. Jawahir. A Review of Surface Integrity in Machining and Its Impact on Functional Performance and Life of Machined Products. Int. J. Sustain. Manuf. 2008; 1 (1/2): 203–236.

[28] Y.B. Guo, W. Li, I.S. Jawahir. Surface Integrity Characterization and Prediction in Machining of Hardened and Difficult-to-Machine Alloys: A State-of-Art Research Review and Analysis. Mach. Sci. Technol. 2009; 13 (4): 437–470.

[29] D. Ulutan, T. Ozel. Machining Induced Surface Integrity in Titanium and Nickel Alloys: A Review. Int. J. Mach. Tools Manuf. 2011; 51 (3): 250–280.

[30] I.C. Noyan, J.B. Cohen. Residual Stress - Measurement by Diffraction and Interpretation, Springer-Verlag, 1987.

[31] E. Brinksmeier, J.T. Cammett, W. König, P. Leskovar, J. Peters, H.K. Tönshoff. Residual Stresses - Measurements and Causes in Machining Processes. Ann. CIRP 1982; 31 (2): 491–510.

[32] F.H. Froes, ed. Titanium : Physical Metallurgy, Processing, and Applications, ASM International, Materials Park, OH, USA, 2015.

[33] M.J.J. Donachie. Titanium - A Technical Guide, 2nd ed., ASM International, Materials Park, OH, USA, 2000.

[34] G. Lütjering, J.C. Williams. Titanium, 2nd ed., Springer-Verlag Berlin Heidelberg New York, 2007.

[35] A.P. Mouritz. Introduction to Aerospace Materials, Woodhead Publishing Limited, 2012.

[36] E.O. Ezugwu, Z.M. Wang. Titanium Alloys and Their Machinability—a Review. J. Mater. Process. Technol. 1997; 68 (3): 262–274.

[37] P.A. Dearnley, A.N. Grearson. Evaluation of Principal Wear Mechanisms of Cemented Carbides and Ceramics Used for Machining Titanium Alloy IMI 318. Mater. Sci. Technol. (United Kingdom) 1986; 2 (1): 47–58.

[38] B. Gunston. Cambridge Aerospace Dictionary, Cambridge University Press, 2004.

[39] E.W. Bartle. Carbon Dioxide Permits Improved Machining Time. Mach. (New York) 1953; 59 (8): 157–158.

[40] Anonymous. Liquid Carbon Dioxide as a Cutting Tool Coolant. Sci. Lubr. 1954; 6 (7): 23–24.

[41] Anonymous. Machining Heat-Resisting Alloys with Carbon Dioxide Coolant. Machinery 1955; 87 (2235): 665–668.

[42] L. Walter. Carbon Dioxide as Cutting Tool Coolant Repays Research with Imposing Savings. Can. Mach. Metalwork. 1965; 76 (8): 94–97.

[43] W.S. Hollis. The Application and Effect of Controlled Atmospheres in the Machining of Metals. Int. J. Mach. Tool Des. Res. 1961; 1 (1–2): 59–78.

[44] J. Kumabe, M. Masuko. Study on Cold Machining (Part 1). Japan Soc. Mech. Eng. - Trans. 1958; 24 (138): 103–108.

[45] Anonymous. Cryogenic Coolants Speed Titanium Machining. Mach. (New York) 1965; 71 (11): 101–102.

[46] K. Uehara, S. Kumagai. Chip Formation, Surface Roughness and Cutting Force in Cryogenic Machining. CIRP Ann. - Manuf. Technol. 1969; 17 (1): 409–416.

[47] Z. Zhao, S.Y. Hong. Cooling Strategies for Cryogenic Machining from a Materials Viewpoint. J. Mater. Eng. Perform. 1992; 1 (5): 669–678.

[48] Z. Zhao, S.Y. Hong. Cryogenic Properties of Some Cutting Tool Materials. J. Mater. Eng. Perform. 1992; 1 (5): 705–714.

[49] Y. Ding, S.Y. Hong. Improvement of Chip Breaking in Machining Low Carbon Steel by Cryogenically Precooling the Workpiece. J. Manuf. Sci. Eng. 1998; 120 (1): 76.

[50] S.Y. Hong, Y. Ding, R.G. Ekkens. Improving Low Carbon Steel Chip Breakability by Cryogenic Chip Cooling. Int. J. Mach. Tools Manuf. 1999; 39 (7): 1065–1085.

[51] S.Y. Hong, Y. Ding. Cooling Approaches and Cutting Temperatures in Cryogenic Machining of Ti-6Al-4V. Int. J. Mach. Tools Manuf. 2001; 41 (10): 1417–1437.

[52] S.Y. Hong, Y. Ding. Micro-Temperature Manipulation in Cryogenic Machining of Low Carbon Steel. J. Mater. Process. Technol. 2001; 116 (1): 22–30.

[53] S.Y. Hong, Y. Ding, W. Jeong. Friction and Cutting Forces in Cryogenic Machining of Ti–6Al–4V. Int. J. Mach. Tools Manuf. 2001; 41 (15): 2271–2285.

[54] S.Y. Hong. Economical and Ecological Cryogenic Machining. J. Manuf. Sci. Eng. 2001;

123 (2): 331.

[55] S.Y. Hong, I. Markus, W. Jeong. New Cooling Approach and Tool Life Improvement in Cryogenic Machining of Titanium Alloy Ti-6Al-4V. Int. J. Mach. Tools Manuf. 2001; 41 (15): 2245–2260.

[56] S.Y. Hong, Y. Ding, J. Jeong. Experimental Evaluation of Friction Coefficient and Liquid Nitrogen Lubrication Effect in Cryogenic Machining. Mach. Sci. Technol. 2002; 6 (2): 235–250.

[57] S.Y. Hong. Lubrication Mechanisms of LN2 in Ecological Cryogenic Machining. Mach. Sci. Technol. 2006; 10 (1):.

[58] G. von Oppen, F. Melchert. Physics for engineers and scientists, Infinity Science Press, Hingham, MA, 2007.

[59] S.S. Gill, R. Singh, H. Singh, J. Singh. Wear Behaviour of Cryogenically Treated Tungsten Carbide Inserts under Dry and Wet Turning Conditions. Int. J. Mach. Tools Manuf. 2009; 49 (3–4): 256–260.

[60] S.L. Truesdale, Y.C. Shin. Microstructural Analysis and Machinability Improvement of Udimet 720 via Cryogenic Milling. Mach. Sci. Technol. 2009; 13 (1): 1–19.

[61] Z.Y. Wang, K.P. Rajurkar. Cryogenic Machining of Hard-to-Cut Materials. Wear 2000; 239 (2): 168–175.

[62] M.J. Bermingham, S. Palanisamy, D. Kent, M.S. Dargusch. A Comparison of Cryogenic and High Pressure Emulsion Cooling Technologies on Tool Life and Chip Morphology in Ti–6Al–4V Cutting. J. Mater. Process. Technol. 2012; 212 (4): 752–765.

[63] F. Klocke, D. Lung, A. Krämer, T. Cayli, H. Sangermann. Potential of Modern Lubricoolant Strategies on Cutting Performance. Key Eng. Mater. 2013; 554–557: 2062–2071.

[64] Y. Ayed, G. Germain, A.P. Melsio, P. Kowalewski, D. Locufier. Impact of Supply Conditions of Liquid Nitrogen on Tool Wear and Surface Integrity When Machining the Ti-6Al-4V Titanium Alloy. Int. J. Adv. Manuf. Technol. 2017; 93 (1–4): 1199–1206.

[65] F. Pusavec, T. Lu, C. Courbon, J. Rech, U. Aljancic, J. Kopac, I.S. Jawahir. Analysis of the Influence of Nitrogen Phase and Surface Heat Transfer Coefficient on Cryogenic Machining Performance. J. Mater. Process. Technol. 2016; 233: 19–28.

[66] S. Cordes, F. Hübner, T. Schaarschmidt. Next Generation High Performance Cutting by Use of Carbon Dioxide as Cryogenics. Procedia CIRP 2014; 14: 401–405.

[67] N. Tapoglou, M.I.A. Lopez, I. Cook, C.M. Taylor. Investigation of the Influence of CO2 Cryogenic Coolant Application on Tool Wear. Procedia CIRP 2017; 63: 745–749.

[68] K. Busch, C. Hochmuth, B. Pause, A. Stoll, R. Wertheim. Investigation of Cooling and Lubrication Strategies for Machining High-Temperature Alloys. Procedia CIRP 2016; 41: 835–840.

[69] S. Sartori, A. Ghiotti, S. Bruschi. Hybrid Lubricating/cooling Strategies to Reduce the Tool Wear in Finishing Turning of Difficult-to-Cut Alloys. Wear 2017; 376–377: 107–114.

[70] A. Bordin, S. Bruschi, A. Ghiotti, P.F.F. Bariani. Analysis of Tool Wear in Cryogenic

Machining of Additive Manufactured Ti6Al4V Alloy. WEAR 2015; 328: 89–99.

[71] S. Sartori, A. Bordin, L. Moro, A. Ghiotti, S. Bruschi. The Influence of Material Properties on the Tool Crater Wear When Machining Ti6Al4V Produced by Additive Manufacturing. Procedia CIRP 2016; 46: 587–590.

[72] S. Sartori, L. Moro, A. Ghiotti, S. Bruschi. On the Tool Wear Mechanisms in Dry and Cryogenic Turning Additive Manufactured Titanium Alloys. Tribol. Int. 2017; 105: 264–273.

[73] S. Sartori, A. Bordin, A. Ghiotti, S. Bruschi. Analysis of the Surface Integrity in Cryogenic Turning of Ti6Al4V Produced by Direct Melting Laser Sintering. Procedia CIRP 2016; 45: 123–126.

[74] A. Bordin, F. Medeossi, A. Ghiotti, S. Bruschi, E. Savio, L. Facchini, F. Bucciotti. Feasibility of Cryogenic Cooling in Finishing Turning of Acetabular Cups Made of Additive Manufactured Ti6Al4V. Procedia CIRP 2016; 46: 615–618.

[75] A. Bordin, S. Imbrogno, G. Rotella, S. Bruschi, A. Ghiotti, D. Umbrello. Finite Element Simulation of Semi-Finishing Turning of Electron Beam Melted Ti6Al4V Under Dry and Cryogenic Cooling. Procedia CIRP 2015; 31: 551–556.

[76] D. Umbrello, A. Bordin, S. Imbrogno, S. Bruschi. 3D Finite Element Modelling of Surface Modification in Dry and Cryogenic Machining of EBM Ti6Al4V Alloy. CIRP J. Manuf. Sci. Technol. 2016; .

[77] Y. Sun, B. Huang, D.A. Puleo, J. Schoop, I.S. Jawahir. Improved Surface Integrity from Cryogenic Machining of Ti-6Al-7Nb Alloy for Biomedical Applications. Procedia CIRP 2016; 45: 63–66.

[78] C. Machai, D. Biermann. Machining of β-Titanium-Alloy Ti–10V–2Fe–3Al under Cryogenic Conditions: Cooling with Carbon Dioxide Snow. J. Mater. Process. Technol. 2011; 211 (6): 1175–1183.

[79] C. Machai, A. Iqbal, D. Biermann, T. Upmeier, S. Schumann. On the Effects of Cutting Speed and Cooling Methodologies in Grooving Operation of Various Tempers of β-Titanium Alloy. J. Mater. Process. Technol. 2013; 213 (7): 1027–1037.

[80] Y. Sun, B. Huang, D.A. Puleo, I.S. Jawahir. Enhanced Machinability of Ti-5553 Alloy from Cryogenic Machining: Comparison with MQL and Flood-Cooled Machining and Modeling. Procedia CIRP 2015; 31: 477–482.

[81] M. Dhananchezian, M. Pradeep Kumar. Cryogenic Turning of the Ti–6Al–4V Alloy with Modified Cutting Tool Inserts. Cryogenics (Guildf). 2011; 51 (1): 34–40.

[82] K.A. Venugopal, S. Paul, a. B. Chattopadhyay. Growth of Tool Wear in Turning of Ti-6Al-4V Alloy under Cryogenic Cooling. Wear 2007; 262 (9–10): 1071–1078.

[83] K.A. Venugopal, S. Paul, a. B. Chattopadhyay. Tool Wear in Cryogenic Turning of Ti-6Al-4V Alloy. Cryogenics (Guildf). 2007; 47 (1): 12–18.

[84] M.J. Bermingham, J. Kirsch, S. Sun, S. Palanisamy, M.S. Dargusch. New Observations on Tool Life, Cutting Forces and Chip Morphology in Cryogenic Machining Ti-6Al-4V. Int. J. Mach. Tools Manuf. 2011; 51 (6): 500–511.

[85] S. Tirelli, E. Chiappini, M. Strano, M. Monno, Q. Semeraro. Experimental Comparison between Traditional and Cryogenic Cooling Conditions in Rough Turning of Ti-6Al-4V.

Key Eng. Mater. 2014; 611–612: 1174–1185.

[86] A. Krämer, F. Klocke, H. Sangermann, D. Lung. Influence of the Lubricoolant Strategy on Thermo-Mechanical Tool Load. CIRP J. Manuf. Sci. Technol. 2014; 7 (1): 40–47.

[87] A. Shokrani, V. Dhokia, S.T. Newman. Comparative Investigation on Using Cryogenic Machining in CNC Milling of Ti-6Al-4V Titanium Alloy. Mach. Sci. Technol. 2016; 20 (3): 475–494.

[88] S.M. Yuan, L.T. Yan, W.D. Liu, Q. Liu. Effects of Cooling Air Temperature on Cryogenic Machining of Ti–6Al–4V Alloy. J. Mater. Process. Technol. 2011; 211 (3): 356–362.

[89] Q.L. An, Y.C. Fu, J.H. Xu. The Application of Cryogenic Pneumatic Mist Jet Impinging in High-Speed Milling of Ti-6Al-4V. Key Eng. Mater. 2006; 315–316: 244–248.

[90] B.D. Jerold, M.P. Kumar. The Influence of Cryogenic Coolants in Machining of Ti–6Al–4V. J. Manuf. Sci. Eng. 2013; 135 (3): 31005-1-31005–8.

[91] G. Rotella, O.W. Dillon, D. Umbrello, L. Settineri, I.S. Jawahir. The Effects of Cooling Conditions on Surface Integrity in Machining of Ti6Al4V Alloy. Int. J. Adv. Manuf. Technol. 2014; 71 (1–4): 47–55.

[92] S. Sartori, A. Bordin, S. Bruschi, A. Ghiotti. Machinability of the EBM Ti6Al4V in Cryogenic Turning. Key Eng. Mater. 2015; 651–653: 1183–1188.

[93] B.D. Cullity. Elements of X-ray diffraction, Addison-Wesley, 1967.

[94] M.E. Fitzpatrick, A.T. Fry, P. Holdway, F.A. Kandil, J. Shackleton, L. Suominen. Determination of residual stresses by X-ray diffraction, National Physical Laboratory, Teddington, UK, 2005.

[95] P.S. Prevéy. X-Ray Diffraction Residual Stress Techniques, in: ASM Handbook, Vol. 10 - Mater. Charact., ASM International, 1986: pp. 380–392.

[96] V. Hauk. Structural and Residual Stress Analysis by Nondestructive Methods, Elsevier Science B.V., Amsterdam, 1997.

[97] M. Ziomek-Moroz. Electropolishing, in: ASM Handbook, Vol. 13A - Corros. Fundam. Testing, Prot., ASM International, Materials Park, OH, USA, 2003: pp. 139–142.

[98] International Organization for Standardization. Tool life testing in milling - Part 1: Face milling (ISO 8688-1), 1989.